Understanding and Evaluating Methods for Assessing Soil Compaction in Agri-food Systems

Amy Sigsworth
Master of Land and Water Systems 2020
The University of British Columbia

Academic supervisor: Dr. Les Lavkulich
Professional supervisor: Dr. Heather Mackay

Abstract

Soil plays a significant role within the hydrological cycle by providing a medium for infiltrating water to be stored in the rooting depth and a conduit for groundwater recharge. Effective infiltration and percolation are imperative in agricultural systems to reduce water erosion and maintain soil quality, enhance water use efficiency by storing water in the rooting zone, foster groundwater recharge which may further service domestic and agricultural water users in the region, and to reduce the effects of heavy rainfall events such as flooding. Infiltration is directly influenced by soil compaction which is a concern in agri-food systems. In order to maintain hydrological functions at the farm scale, as well enhance productivity, land managers commonly assess soil compaction in production fields. However, current tools, such as the Soil Compaction Tester (SCT), are not efficient in assessing spatial variability at the farm scale. This project evaluated ground-penetrating radar (GPR) as a method of assessing soil compaction in both cultivated and non-cultivated fields. The GPR results were compared to results from the SCT and soil analysis from core samples. The results demonstrated the potential for GPR as an efficient technique in assessing compaction at the field scale in certain circumstances and soil textures. Further research is recommended in larger scale and more established production systems to test the method's efficiency in assessing soil compaction and spatial variability.

Table of Contents

ABSTRACT **2**

LIST OF FIGURES **4**

INTRODUCTION **6**

Background 10
Thesis statement 14
Research objectives 14

METHODS AND MATERIALS **15**

Literature review 15
Field study 15

RESULTS AND DISCUSSION **21**

Analysis of literature 21
Field study 22
Scope and Limitations 30

RECOMMENDATIONS **30**

Ground-penetrating radar 30
Future research 31

CONCLUDING REMARKS **31**

REFERENCES **32**

ACKNOWLEDGEMENTS **35**

APPENDICES **36**

Appendix A 36
Appendix B 37
Appendix C 38
Appendix D 41
Appendix E 42

List of Figures

Figure 1. The hydrological cycle 5
Figure 2. Illustration of soil compaction 8
Figure 3. Map of the Fraser-Nooksack Lowland 9
Figure 4. Elevation map of Fraser-Nooksack Lowland with major river systems 10
Figure 5. Illustration of penetrometer
Figure 6. Map of field site 14
Figure 7. Site A (left) and site G (right) 15
Figure 8. Field measurement design for site A and G 16
Figure 9. Portion of A6 transect radargram 23
Figure 10. Portion of G1 transect radargram 23
Figure 11. Radargram showing compaction in G1 24
Figure 12. Radargram showing compaction in G6 24
Figure 13. Compaction and signal attenuation in G6 24
Figure 14. Soil compaction, rock, and pipe in G6 25
Figure 15. Example of little compaction in A3 26
Figure 16. GPR error 26
Figure 17. PCA of field measurement dataset 28
Figure 18. Climate normals from 1981 to 2010 at Vancouver International Airport Station. 34
Figure 19. Site map with transects. 35

List of Tables

Table 1. Mean and median penetrometer readings 22
Table 2. Physical soil properties and organic matter content at site A and G 27
Table 3. Electromagnetic properties of earth materials 34
Table 4. Penetrometer readings for site G. 36
Table 5. Penetrometer readings for site A. 37
Table 6. Site G soil moisture and bulk density measurements 39
Table 7. Site A soil moisture and bulk density measurements 39

Introduction

Agricultural production, whether rain-fed or irrigated, is eminently dependent on the hydrological cycle which describes the circulation of water as it transitions through various states (i.e. solid, liquid, gas) among the atmosphere, biosphere, hydrosphere and cryosphere (Rast et al., 2014). The components of the cycle include evaporation and evapotranspiration, precipitation, runoff, interception, infiltration and percolation, and storage. As observed in Figure 1, a schematic illustration of the cycle through a landscape, infiltration and percolation are two important components of the cycle for water storage—a vital feature of crop production. During a rainfall event, water droplets that hit the ground may infiltrate the soil, without surface runoff, if the infiltration rate is greater than the intensity of precipitation. Water that infiltrates the soil can remain stored in the rooting zone as green water (i.e. water stored in soil or vegetation) or percolate into subsurface material eventually reaching groundwater as blue water (i.e. freshwater stored as reservoirs) (Sood et al., 2014). Infiltration therefore provides numerous benefits such as 1) replenishing water into the rooting zone, 2) recharging groundwater, 3) reducing the potential for erosion by water, and 4) reducing the potential effects of heavy rainfall such as flooding.

Figure 1. The hydrological cycle. Source: (Rast et al., 2014)

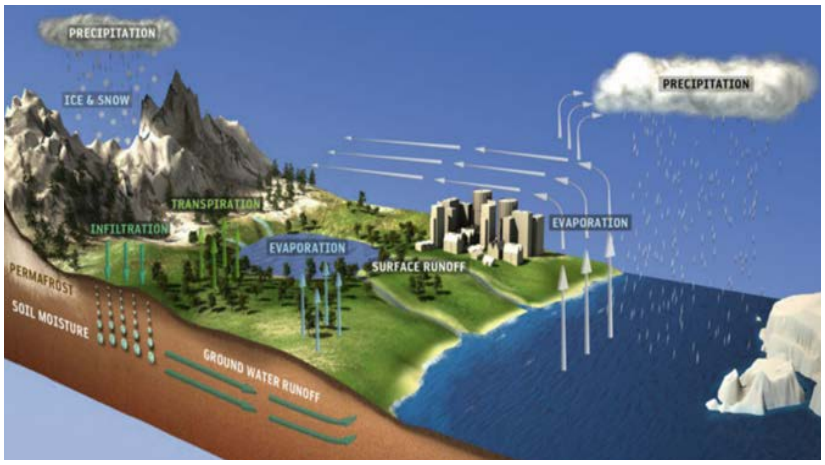

Due to both a growing global trend in agricultural intensification and a changing climate in which greater climatic variability and more severe precipitation events are predicted (Trenberth, 2011; Pendergrass & Hartmann, 2014), enhancing and safeguarding the resiliency of agricultural production systems is essential in order to sustain productivity and global food security. A significant component of agricultural crop production is soil quality. Physical soil characteristics are one component of soil quality and are related to intrinsic properties (e.g. mineral types and grain size) but may also be heavily influenced by management practices and climate (e.g. bulk density, porosity, percent organic matter). Soil physical properties are also correlated to water use in crop production as infiltrated water can be stored in the rooting zone and available for plant uptake (Sood et al., 2014), thereby reducing irrigation requirements. Therefore, especially

pertinent in a changing climate, adjusting management practices to mitigate soil compaction and improve water use and efficiency is imperative.

Soil compaction is most notable in agricultural systems as a result of mechanical pressure leading to the collapse of soil structure and loss of macroporosity, effectively increasing bulk density (Alaoui et al., 2018). However, compaction may result from both natural processes (e.g. freeze-thaw cycles) and anthropogenic practices (e.g. the use of heavy machinery) (Nawaz et al., 2013). Five types of soil compaction have been identified in non-urbanized environments; these include: 1) general compaction caused by external loads or from soil sloping and hard setting, 2) local compaction from the use of implements or tires, 3) subsoil compaction below the tillage depth, 4) secondary compaction arising from surface loadings on a structurally weak soil layer above a compacted layer, and 5) compaction formed by natural cementation or from natural clay pans (Spoor, 2006). Despite the various types and causes of soil compaction, agricultural production systems are most concerned with reducing compaction developed through management practices; this is especially a concern as the risk of soil compaction increases with agricultural intensification as greater production generally requires more frequent use of heavy machinery (Hemmat & Adamchuk, 2008). Moreover, inherent soil characteristics such as organic matter, water content, soil structure and texture further impact the potential for compaction by heavy machinery (Nawaz et al., 2013).

Compaction affects several natural processes that are integral to agricultural production, the hydrological cycle, and ecosystem function (Alaoui et al., 2018; Hemmat & Adamchuk, 2008). As previously stated, soil physical properties influence the infiltration of water. Soil compaction indicated directly by the metric of dry bulk density, reduces the efficiency of water to infiltrate soil as hydraulic conductivity is minimized (Brady & Weil, 2010). During an intense precipitation event, water that does not infiltrate the soil moves as overland flow, thus increasing both the susceptibility of soil to erosion by water (Brady & Weil, 2010) and the potential for runoff of agrochemicals to pollute surface water (Alaoui et al., 2018; Hemmat & Adamchuk, 2008). Reduced infiltration also impacts agricultural production as soil acts as an important source of water storage; soil that is not effectively storing water will have additional irrigation requirements or face potential yield loss. In addition, soil compaction may also impede the growth and penetration of roots, the aeration of soil, and the ability of plants to uptake water (due to increased matric potential) (Brady & Weil, 2010), which can result in substantial yield loss. Furthermore, the consequences of reduced infiltration from soil compaction has the potential to go beyond the farm scale (i.e. crop production, land degradation) and affect the greater hydrological cycle by impacting groundwater recharge potential. The permeability of soil and subsoil greatly influence groundwater processes (Healy & Scanlon, 2010); in the case where soil is compacted at the surface, the ability for water to infiltrate and percolate subsurface materials is minimized thus reducing groundwater recharge (Healy & Scanlon, 2010). This is not only concerning at the level of agricultural production when it is dependent on irrigation water from a groundwater source, but also for other local user groups such as domestic users who are reliant on groundwater to meet daily water demands. Furthermore, deficiencies in the water level of an aquifer may go beyond

user groups and affect ecosystem functions. For example, fish-bearing streams may rely on groundwater for minimum baseflows during dry seasons.

The ability of water to effectively infiltrate and percolate through soil also impacts the evaporation and evapotranspiration (ET) in the greater hydrological cycle. In the case of a light rain event, water that has made its way to bare soil will likely be completely lost to evaporation as it is directly exposed to radiant energy (Balugani et al., 2017). Water that does infiltrate the rooting zone may also be quickly lost to ET creating a moisture gradient between the upper unsaturated zone and lower saturated water table. This gradient leads to the ET of subsurface green water as water fluxes pull moisture upwards towards the unsaturated zone, further depleting groundwater storage and minimizing groundwater recharge (Balugani et al., 2017). Similarly, in areas in which soil compaction minimizes the rate of infiltration, water may be lost to evaporation, therefore reducing both the volume of green water stored in the rooting zone and the amount of water recharging groundwater.

Land use may play a significant role in modifying hydrological dynamics (Alaoui et al., 2018) as a result of management implications on bulk density and porosity. In cases where land management effectuates modified infiltration, cascading effects may result in low soil moisture in the rooting zone and groundwater depletion over time. When compared to a soil of the same type, uncompacted soil infiltrates water faster than a massively compacted one (Nawaz et al., 2013). When the rate of precipitation is greater than the rate of infiltration, water may begin to move as overland flow, increasing the risk of soil erosion by water (Alaoui et al., 2018). Thus, consideration of both land-use type and management approaches in agricultural systems are integral to maintaining hydrological functionality.

The level of soil compaction has an effect on evaporation, an important component of the hydrological cycle. After a precipitation event, water that does not effectively infiltrate the soil is stored as surface water (e.g. puddles or overland flow to a body of water) or in the upper layer of the rooting zone. This water is more likely to be lost to evaporation as it is exposed to radiant energy. In areas where soil compaction impedes infiltration, increased evaporation may cause a change in the microclimate by increasing water vapour in the atmosphere. Evaporation increases the volume of water vapour in the atmosphere which is an effective greenhouse gas that contributes to global warming. Although the potential for increased evaporation as a result of soil compaction in relation to both water storage and agricultural microclimates is an important issue worth exploring, this study will only be concerned with the impact of soil compaction on the hydrological components infiltration and percolation in relation to plant available water and groundwater recharge.

Bulk density can be used as a direct estimator of soil compaction at a site. Determining dry bulk density, defined as the mass of a unit volume of dry soil (Brady & Weil, 2010), using the core method is common for quantifying the level of soil compaction (Nawaz et al., 2013). Generally speaking, the bulk density of soil will increase as a result of collapsed macropores (Figure 2). A decrease in macropores and their connectivity generates a loss of tortuosity, and ultimately slows

down the infiltration and percolation of water (Nawaz et al., 2013). Thus, changes in bulk density can aid in predicting how land use is affecting the hydrological cycle.

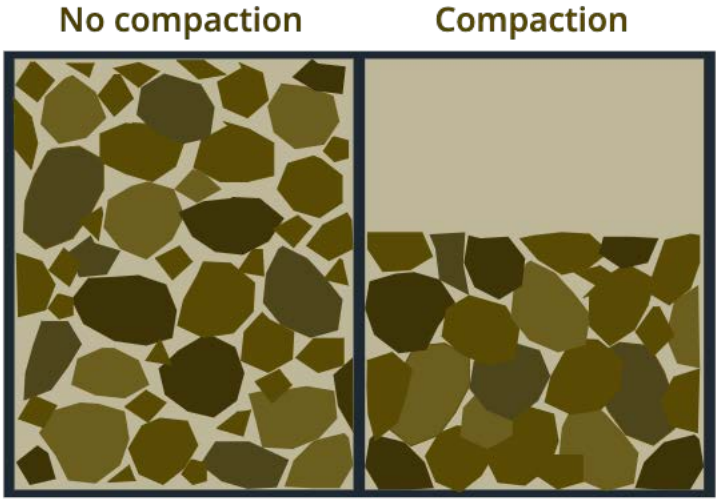

Figure 2. Illustration of soil compaction and the difference in porosity in a non-compacted (left) and compacted (right) soil. The non-compacted soil has a lower bulk density compared to the compacted soil of the same texture and organic matter content due to a larger prevalence of macropores.

The impacts that a land-use has on bulk density are not spatially uniform; the level of compaction in a production system is variable due to difference in inherent soil characteristics, topography, and management practices. For instance, choice of tillage treatments may impact the risk of compaction (Bogunovic et al., 2018). Additionally, land-use type is also related to the risk of compaction, where the risk increases with the use of heavy machinery (Batey, 2009), which also contributes to spatial variability within a production landscape.

The variability of compaction at a site is an important consideration when developing land management mitigation strategies to improve groundwater recharge and soil water storage for agricultural production. Methods such as penetrometer resistance[1] are widely available to assess compaction at a single point (Duiker, 2002; Hemmat & Adamchuk, 2008); however, this method is not feasible for a full assessment of spatial variability as numerous distinct readings across a field are necessary and would require considerable time. Similarly, although bulk density is a direct metric for estimating soil compaction, it requires significant labour and time to collect samples and is considered a destructive method as it disturbs the surrounding soil. To develop an effective assessment of compaction at the farm-scale, appropriate and efficient techniques must be utilized to accurately evaluate both soil compaction and its spatial variability to enhance agricultural productivity as climate change has and continues to impact water resources (Trenberth, 2011).

[1] Also referred to as cone penetrometer and soil compaction tester

Background

Study context

Figure 3. Map of the Fraser-Nooksack Lowland highlighting its cross-national boundary. Source: (Buckley et al., 2015)

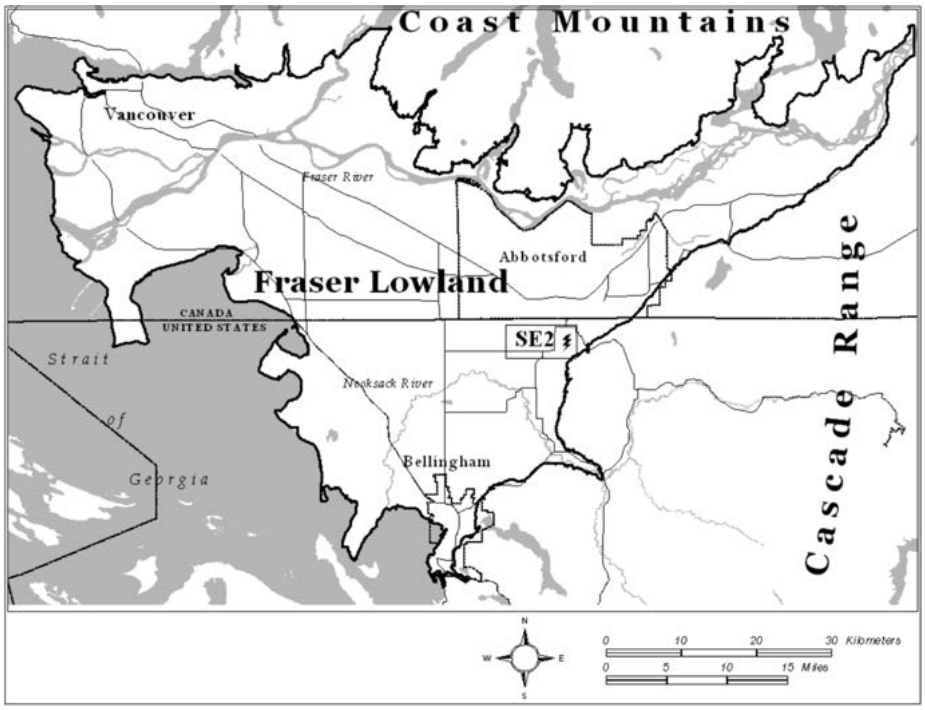

The area under investigation is the Fraser Lowland, a physiographic region of the Pacific Northwest that includes the Lower Mainland of British Columbia and Whatcom county of Washington (see Figure 3) (Buckley et al., 2015). The region comprises two major river systems, the Fraser and Nooksack (Figure 4). The Fraser drainage basin includes the Coast Mountains region with discharges entering the Strait of Georgia, with the Nooksack draining from the North Cascade Range and discharging into Bellingham Bay (see Figure 4) (Kovanen & Slaymaker, 2015). The climate is defined as moderate and rainy with an average temperature of 10.4°C and annual precipitation of 1190 mm from 1981 to 2010[2]. The region maintains several water sources including reservoirs and aquifers. However, aquifers in the Fraser-Nooksack are both being depleted and facing anthropogenic contamination. Additionally, the region faces summer water deficits that may impact agricultural production systems. It is therefore important for land managers to optimize groundwater recharge and to optimize soil water storage on their land to maintain ecological function and production systems.

[2] Refer to Figure 18 in Appendix A for more information on local climate normal from the Vancouver Int'l airport.

Figure 4. Elevation map of Fraser-Nooksack Lowland with major river systems.
source: (Kovanen & Slaymaker, 2015)

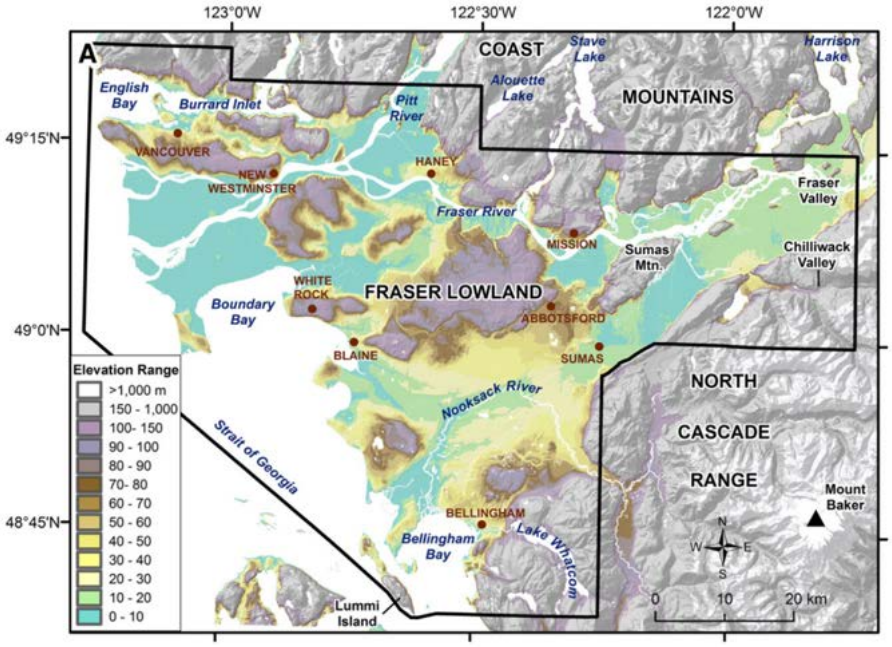

Ground-penetrating radar[3]

A technique called ground-penetrating radar (GPR) has been proposed as a rapid method to determine soil compaction and spatial variability on a wide scale. However, an in-depth evaluation of GPR and its feasibility in assessing compaction and spatial variability has not yet been conducted.

GPR uses electromagnetic (EM) pulses to detect changes in a medium. The system functions by radiating EM pulses (with possible frequencies ranging from 10 MHz to 3.5 GHz) from a transmitter antenna which penetrates a medium and returns to a receiver antenna where the information is transferred to a device for storage (Carrick Utsi, 2017). A radargram is produced from the signals acquired as the EM waves pass through a medium; when it encounters a boundary or a material with a different dielectric constant (E), a signal is returned to the receiver, thus producing a visual change in the radargram. Materials have varying E values[4] resulting in energy reflections observed as hyperbolas or boundaries in a radargram. The larger the difference in E between materials, the more intense the GPR signal within the radargram; this is mathematically referred to as the reflection coefficient (R) (equation 1). Additionally, the receptor utilizes the time required for a signal to return as a measure of depth.

[3] The information in this section was collected from a webinar by Greg Johnston at Sensors and Software.

[4] See Table 3 in Appendix A for electromagnetic properties of earth materials.

Equation 1

$$R = \frac{\sqrt{E_1} - \sqrt{E_2}}{\sqrt{E_1} + \sqrt{E_2}}$$

If E_1 and E_2 are similar in value, most of the wave will transmit through the interface. For example, in the case of a wave moving through a medium of dry sand (E1= 3) in which a granite rock (E2=6) is embedded, only approximately 5 percent will be reflected with 95 percent transmitting through the rock, resulting in a very weak reflecting boundary on the radargram. If pore space within a sandy medium is filled with air (E= 1), there will be very little reflection as the contrast in E is low; however, if the pore is filled with water (E= 80), a strong reflection will occur. The presence of water in soil therefore has the largest overall effect of the bulk E value of the soil. GPR radargrams need to be interpreted not in terms of objects embedded into the soil, but rather as reflections produced from contrasts in E. Thus, the strength of a hyperbola, which is formed when a GPR EM wave crosses over a point target, is due to the contrast between the material and the surrounding soil. Weak hyperbolas will have a similar E as the surrounding soil.

The depth that the EM wave will propagate before it is absorbed or attenuated is dependent on the E of the material. Waves may be attenuated before reaching the receiver if the object is too far away or if the E of the soil is high (in which case the soil absorbs most of the wave and its reflection). Soils generally have high E and absorb the signal quickly. If a boundary is present at depth, it may be invisible to the GPR; in this case, the EM wave will reach the boundary and reflect but will be absorbed and attenuated by the surrounding soil before reaching the receiver. Soils high in clay as well as saturated soils have naturally high E and may provide poor quality GPR radargrams.

Surface bands at the top are from differences in the E from air to soil. When the transmitter fires, the first signal to return to the receiver is from the signal travelling through the air at 0.3 m/ns (speed of light) and is referred to as the direct airwave. This is the first band seen in the radargram. After which the direct groundwave is the second signal to arrive. Together these are called direct arrivals; they generally emerge as three bands due to interference with one another, thus appearing as an individual event. The direct arrivals are visualized as high amplitude bands at the top of the radargram and can mask shallow and surface compaction. However, this can be mitigated by using a filter when processing the data to subtract background noise.

The bottom of the radargram contains radiofrequency (RF) noise. At this depth, the GPR signals have been attenuated. The RF noise comes from intervening energy waves being picked up by the GPR receiver. This noise can be ignored.

GPR cannot show the composition of subsurface material; rather it determines its structure. Composition may be interpreted and inferred based on the data and contextual information from the site. Thus, the interpretation of soil composition in terms of saturation, mineral composition, embedded materials can only be speculated based on interpretation, but not known for certain

without using destructive techniques. However, since soil compaction is a structural phenomenon, GPR may be used to detect differences in structure between strata and within the medium. Geophysical context is important for strengthening interpretation of GPR data.

Penetrometer

The penetrometer, otherwise known as a soil compaction tester, is a piece of equipment that is used as a diagnostic tool to estimate both the extent and depth of soil compaction. It provides an empirical measurement of the soil state as a representation of the net effect of soil properties (i.e. bulk density, dry specific volume, void ratio, and porosity) (Hemmat & Adamchuk, 2008). The tool consists of a graded shaft attached to a reading scale. A 30-degree stainless steel cone is attached to the tip of the shaft. Two sizes of cones are available depending on the soil type; the larger ¾ (base diameter in inches) tip is intended for use in soft soils and the ½ tip for harder soils. The reading scale indicates measurements in pounds per square inch (psi), and the scale read is dependent on the size of the cone tip used, with the outer reading representing the ¾ tip and the inner reading representing the ½ tip (see Figure 5).

The penetrometer functions by simulating the pressure of root growth through soil and therefore provides an indicator of compaction with respect to crop growth. A reading of over 300 psi indicates practically no possible root penetration and thus suggests compaction at the location (Duiker, 2002). However, this reading does not imply that absolutely no root may penetrate the soil at the location as there may be natural cracks and spatial variability.

The penetrometer reading (indicated as the cone index) may be used to assess the overall compaction of a site when numerous readings are taken. In this case, the percent average measuring points with a cone index of >300 psi can be calculated to determine the level of compaction: <30% indicates little to no compaction, 50–75% indicates moderate compaction, and >75% indicates severe compaction (Duiker, 2002).

Figure 5. Illustration of penetrometer. Photo courtesy of Dickey John

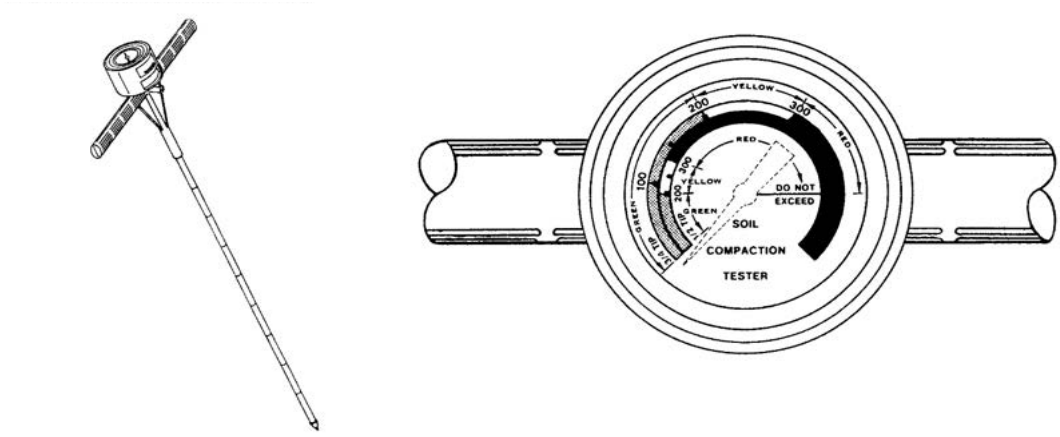

Although the penetrometer is a simple, cost-effective, and standardized tool, it does encompass several limitations. To obtain an accurate reading, the shaft must be inserted into the

soil at a constant speed which may be difficult to achieve manually. Additionally, if the goal is to assess spatial variability, measurements at multiple points must be taken which can be time-consuming and costly (Hemmat & Adamchuk, 2008).

Thesis statement

There is a need for an effective method for assessing spatial variability regarding soil compaction in agricultural systems in areas at risk of water deficits as climate norms shift and demand for agricultural production grows. This report provides a feasibility study using GPR for assessing spatial variability by conducting an integrated method evaluating soil compaction at a known site to further assist agrologists and land managers in mitigating and attending to soil compaction in production systems.

Research objectives

The final report will aim to meet the following objectives:

1. Provide a literature review of studies assessing GPR and penetrometer resistance in relation to spatial variability of soil compaction.
   - Studies that have explored and compared GPR and penetrometer assessments of soil compaction will be reviewed and summarized. However, there are currently no relevant studies that have been conducted specifically on soil types of the Fraser-Nooksack Lowlands. This literature review will act as a guide to the field study.

2. Conduct a field study for evaluating soil compaction and possible spatial variability in an agri-food system using an integrated approach by collecting field measurement data using ground-penetrating radar (GPR), penetrometer resistance, and core samples for laboratory analysis to begin calibration for future research in the Fraser-Nooksack Lowland.
   - This qualitative field study will aim to collect data regarding compaction at two sites (cultivated and uncultivated) to begin an assessment of possible methods that can accurately and cost-effectively measure soil compaction at different spatial scales of interest in the soils and production systems that are present in the Fraser-Nooksack Lowlands. This work aims to assist land managers by developing methods to assess and mitigate compaction and ultimately improve production systems by optimizing water use.

3. Assess the accuracy, feasibility, and cost of GPR technology as a possible tool for evaluating and maintaining appropriate physical soil quality in the Fraser-Nooksack Lowlands.

Methods and Materials

Literature review

Studies regarding the assessment of soil compaction by GPR were collected from the University of British Columbia research commons. Keywords searched included: ground-penetrating radar, GPR, soil compaction, porosity, infiltration, and soil bulk density.

Field study

A field test was conducted in order to meet objective 2. The field measurements were collected to compare information regarding characteristics of soil compaction at two sites, one cultivated and one uncultivated, utilizing two indirect methods (penetrometer and GPR) and one direct method (dry bulk density) as indicators of soil compaction. All three techniques were replicated at each site.

Study site

Figure 6. Map of the study area. site highlighting the location of the two field sites at Totem Field at the University of British Columbia, Vancouver, Canada. Courtesy of Google Earth Pro.

The two sites were located at Totem Field at the University of British Columbia, Point Grey campus (see Figure 6). The soil texture at the site is sandy loam with an estimated organic matter content of 4% (G. Healy, personal communication, 2020).

Figure 7. Site A (left) and site G (right)

Two plots were chosen at Totem field to represent both a cultivated (disturbed) and uncultivated (undisturbed) site. The agriculture (A) and grass (G) sites were similar in elevation with 80 m and 79 m above sea level respectively. Site A had loose soil which had recently (*ask Glen for date) been tilled and amended with organic matter (ask glen what type). The site was observed to have tractor tire passes as can be seen in Figure 7. Both sites measured 15 X 42 meters with 3 meters spacing between a total of 6 transects lengthwise[5]. Field measurements (GPR scan, penetrometer readings, and core samples) were collected along each of the six transects per site.

[5] Refer to Figure 19 in appendix B for a google earth map of the sites with transects.

Figure 8. Field measurement design for site A and G. This is a schematic illustration of the field design and location of measurements for site A represented by lines A1 to A6, and site G, represented by lines G1 to G6. The numbers outlined represent the distance in meters. The pink lines running lengthwise represent the path of the GPR reading. Red dots indicate a cone index reading from the penetrometer. Red and yellow dots represent the location of a core sample taken.

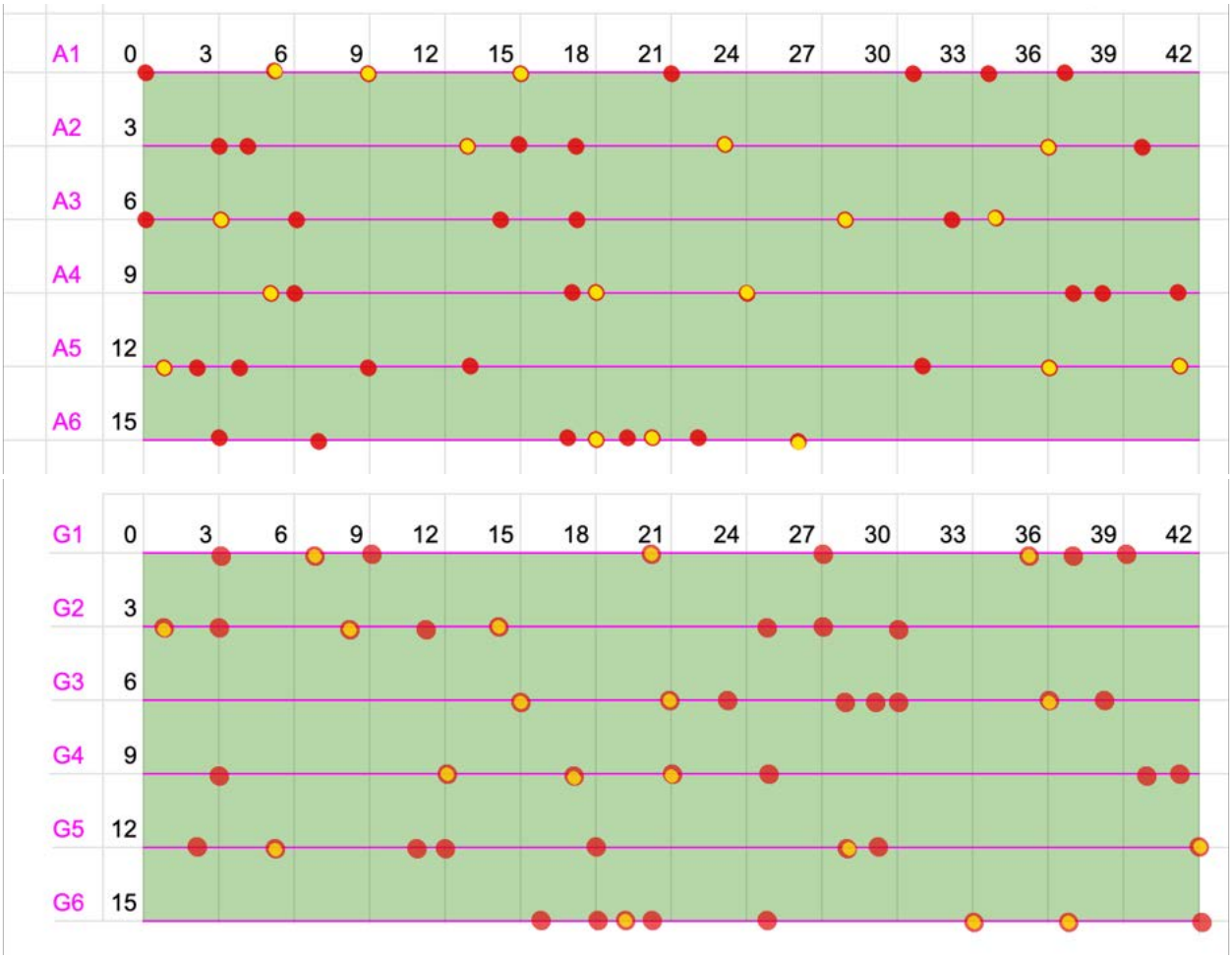

Penetrometer

The soil compaction tester (i.e. penetrometer), manufactured by the Dickey-John Corporation, employed the ½ inch tip which has a pressure range of 0-600 psi[6]. The penetrometer was inserted in the soil at a constant speed (~2.5 cm per second). The grooves along the shaft in increments of 3 inches (~7.6 cm) assist as markers for assessing depth. For this study, a cone index reading was taken at the first 4 grooves when the marker was approximately aligned with the surface of the soil. Readings were taken at the approximate depths of 7.6 cm, 15.2 cm, 22.9 cm, and 30.5 cm within a location. Eight random locations were selected per transect for readings using an online number generator, resulting in 48 locations per site with cone index readings recorded at four depths per location. Figure 8 illustrates the locations of penetrometer readings at both sites.

[6] More information about the soil compaction tester can be found at http://www.dickey-john.com/support/soil-compaction-tester/

The cone index values at each location were processed somewhat arbitrarily by modifying compaction categories developed by Murdock et al. (1993). A compaction reading value was given to each location by the following equation:

Equation 2

$$C = \frac{(\sum x_i)}{n}$$

Where $\sum x_i$ is the sum of the cone indexes and n is the number of readings per location.

If $C < 200$, there is little to no compaction

If $200 < C < 250$, there is slight to moderate compaction

If $C > 300$, there is severe compaction

Locations where penetrometer readings were taken were superimposed onto the corresponding radargram with a green arrow indicating little compaction, a yellow arrow for moderate compaction, and a red arrow for severe compaction.

Ground-penetrating radar

A Proceq portable GPR device was rented from Hoskin Scientific LTD (model: G-896-GPR Live) and provided a radar antenna range of 0.9 to 3.5 GHz. The measuring presets were adjusted as follows:

- Measuring mode: Line scan
- Resolution: Max depth
- Repetition rate (scans/cm): 1.0
- Units: Metric

The GPR was pushed across six 42 m transects in both the A and G sites[7]. As one member pushed the GPR forward following the premeasured line, another followed while observing the real-time radargram produced on the associated Proceq application for Ipad.

[7] Refer to figure 19 in appendix B for a map showing the approximate outline of the transects followed for the GPR data collection.

Soil property measurements

Soil cores were collected at three locations per transect, where penetrometer readings had been taken to compare the results. Areas where soil cores were taken can be visualized in Figure 8 by the yellow circles. Two depths (~10 and ~20 cm) were sampled from each location using a ring with a diameter of 5.3 cm and a height of 2.9 cm. The cores were gently inserted and tapped into the soil vertically using the edge of a wooden block and efforts were made to minimize compaction of the sample. A total of 72 soil samples were collected from both sites.

Dry bulk density:

Soil samples were weighed then dried in a conventional oven at 105°C for up to 24 hours (or until the samples reached a constant weight). The dry samples were weighed again to calculate dry bulk density:

Equation 3

$$\rho_b = \frac{M_s}{V_t}$$

Where M_s is the mass of the dry solids in grams and V_t is the volume of the ring in cm^3.

Gravimetric water content:

Gravimetric water content was calculated using the weight of dry and wet samples:

Equation 4

$$\theta_g = \frac{m_{water}}{m_{soil}} = \frac{m_{wet} - m_{dry}}{m_{dry}}$$

Where m_{water} is the mass of the wet sample is grams, and m_{soil} is the mass of the oven-dried sample in grams.

Soil organic matter content:

After drying, samples from one location per transect were randomly selected to be processed for organic matter content. Two depths (~10 cm and ~20 cm) per location were assessed. The loss-on-ignition (LOI) method was chosen as research has found it to be an adequate method for estimating percent organic matter (Hoogsteen et al., 2015). A total of 24 samples were weighed

and placed in a muffle furnace at 350°C for 3 hours followed by 500°C for 6 hours, with the samples being weighted again after each event.

LOI estimates soil organic matter (SOM) by considering gravimetric changes in a sample after being exposed to high temperatures resulting in the oxidation of organic material, leaving behind only the inorganic fraction (i.e. ash) (Nelson & Sommers, 1996). The percent organic matter for each sample was estimated using the following equation:

Equation 5

$$\%\, OM — LOI(350) = \frac{m_{dry} - m_{ash}}{m_{dry}} \times 100$$

Carbon stocks:

Carbon stocks were estimated in each sample by first multiplying the mass of the weight loss from the LOI(350) ($m_{dry} - m_{ash}$) by the generally accept carbon content in SOM coefficient of 0.58 (Jensen et al., 2018), followed by dividing the C content by the sample dry weight resulting in the mass fraction (fc). The carbon stock was then calculated as follows:

Equation 6

$$c_s = f_c \rho_b V$$

Where f_c is the mass fraction of C in the dry mass, ρ_b is the dry bulk density, and V is the volume of the sample (Gifford & Roderick, 2003).

Principal Component Analysis

A principal component analysis (PCA) was carried out using the data collected from field measurements. PCA is a multivariate[8] and dimension reduction[9] technique used to analyze and draw out patterns in complex datasets (Abdi & Williams, 2010). This type of statistical analysis finds the data with the most variance and represents it as a new orthogonal variable referred to as a principal component which can then be displayed as points on a map to highlight patterns of similarity (Abdi & Williams, 2010).

A PCA plot converts the covariance among points into a 2D graph in which highly correlated points cluster together. This is done by singular value decomposition (SVD) in which

[8] Method used to measure the relationship between two or more variables.

[9] Process of reducing the dimensions of a dataset to present the data in a more meaningful way.

the values are scaled and centred to provide a visualization of how points vary around the origin (0,0). The data is centred by calculating the correlation coefficient s_{XY} (based on covariance)

Equation 7

$$s_{XY} = \frac{\sum_{i=1}^{n} (X_i - \underline{X})(Y_i - \underline{Y})}{n - 1}$$

The observations are then scaled using the correlation coefficient and the standard deviation (SD) to allow the axis to be representable of the total variation.

Equation 8

$$r_{XY} = \frac{S_{XY}}{s_X \cdot s_Y}$$

The axes are ranked among the order of importance with principal component 1 (PC1) displaying the points with the largest variance. Thus, the principal components are axes that best explain variation in data against properties of the data (e.g. agricultural site versus grass site). In the PCA biplot, the points denote individual samples and the arrows represent the variables; the biplot shows the correlation structure between different variables where the loadings (i.e. arrows) represent the correlation (i.e. loading vectors of similar length and direction equal high correlation).

PCA was used as an exploratory data analysis using the large dataset collected from the field measurements in the field study. The variables used in the PCA include the following collected field measurements from site A and G: penetrometer reading at 7.6 cm, 15.2 cm, 22.9 cm, and 30.5 cm, depth to compaction according to GPR scan interpretation, gravimetric water content, and carbon stocks.

Results and Discussion

Analysis of literature

Freeland, Sorochan, Goddard & McElrroy evaluated soil compaction of a football turfgrass field using GPR complemented by data obtained from the Clegg Impact Soil Tester (CIST), a common tool used in the industry that indirectly estimates compaction (2008). The GPR with an ultra-high frequency antenna was towed along on a plastic skip by an electric golf cart to collect data along multiple transects within the field located in Knoxville, Tennessee at Neyland Stadium. The objective of the study was to develop a reliable and efficient method of gathering compaction

data while simultaneously conducting routine maintenance such as mowing and fertilizing. Freeland et al. found that the GPR scans complemented the more laborious CIST data and concluded that GPR could be implemented as an efficient strategy for monitoring soil compaction within a football turfgrass field (2008).

In a study by Wang, Hu, Zhao & Li, the relationship between soil compaction and GPR data was investigated by analyzing penetrometer resistance, bulk density, and GPR signals under different conditions (2016). They found a significant correlation between the EM wave velocity and dry bulk density; as bulk density increases, there is a change in water content that influenced the GPR signals due to a change in water behaviour within the soil (from free water to bound water). Additionally, the results showed a connection between high penetrometer cone indexes and GPR signals with low amplitude and a fast decay rate back to noise level (Wang et al., 2016). However, to date, the quantification of soil compaction and GPR signals have not been statistically analyzed, leading to questionable reliability and uniform assessment of soil compaction using GPR.

Akinsunmade, Tomecka-Suchon, & Pysz investigated the relationship between GPR signals and soil properties in regard to the impact of tractor passes in a predominantly sandy-loam cultivated field located in Krakow, Poland (2019). The objective of this study was to understand how GPR signals and soil degradation are related. The results showed a change in reflection coefficient and GPR wave velocity between scans taken pre and post tractor passes within the study site. Thus, a relationship was established between penetrometer resistance due to changes in porosity and changes in the reflection coefficient and wave velocity of GPR signals. The study cited the use of GPR as a simple method for assessing and tracking changes in physical soil properties.

There are limited peer-review studies regarding the evaluation of GPR as a method for assessing soil compaction in agri-food systems; however, information collected from previous studies summarized above suggest that GPR has the potential to be a useful tool for land managers at it may accurately depict changes in physical soil properties in particular soil types.

Field study

Site history

The historical context of land use at a study site is an important precursor to the interpretation of field measurements. The land cover history of Totem Field was explored using Google Earth Pro. Satellite images of the field were irregularly updated but spanned from August 2003 to June 2019. It was observed that both the agriculture and grass site were maintained as lawn grass until the 2016 growing season in which the agriculture field was first tilled and used for cultivation; this was confirmed by the Field Technician (G. Healy, personal communication, 2020). Additionally, the tree cover area located at the northern end of the grass field was cultivated at some point between 2011 and 2013.

Penetrometer

Penetrometer readings[10] from the agricultural site indicated little to no compaction (cone index readings of <250 psi) to a depth of 15 cm for both site A and G; however, site G found a higher degree of compaction at individual points with more frequent readings of ≥250 psi, resulting in a higher mean value within that depth range (see Table 1 for comparison). Both sites contained moderate to severe compaction at the depth range of 15-30 cm with mean values ≥250 psi, although the grass site had considerably more individual readings ≥300 psi. This is likely explained by site management as the agriculture site had recently been plowed (plow depth ~20 to 30 cm) and the grass margin is regularly mowed by a tractor which may impact the degree of soil compaction through multiple soil horizons.

Table 1. Mean and median penetrometer readings

Site	***Depth range***	***Mean****	***Median***
Agriculture	0-15 cm	124 ± 67	125
	15-30 cm	266 ± 81	300
Grass	0-15 cm	206 ± 88	200
	15-30 cm	299 ± 4	300

*Values denote mean ± 1SD.

Ground-penetrating radar[11]

The GPR radargrams were processed using the Proceq application downloaded to an iPad. The images were adjusted as follows:

- Linear gain (dB): 28
- Time gain compensation (dB/m): 74
- Dielectric constant (E): 13.1
- Display: Seismic

The radargrams illustrated some differences between the two study sites. A greater degree of structural homogeny was inferred from the GPR results within the grass site. This can be visualized by comparing the degree of reflections from both sites in Figures 9 and 10. Transect A6, as represented in Figure 9, displays stronger reflections illustrated by the dark bands present;

[10] Refer to Appendix C for raw penetrometer reading data corresponding to both the agriculture and grass sites.

[11] Complete transect radargrams are available in Appendix E.

whereby transect G1, as represented by Figure 10, has fewer strong reflections. Since little moisture differences were found between the sites[12], these reflections could imply structural changes in the soil medium. Further strengthening this possibility is the penetrometer results which displayed a larger degree of soil compaction throughout the soil depths tested in the grass site whereby the agriculture site showed more spatial variation.

Figure 9. Portion of A6 transect radargram

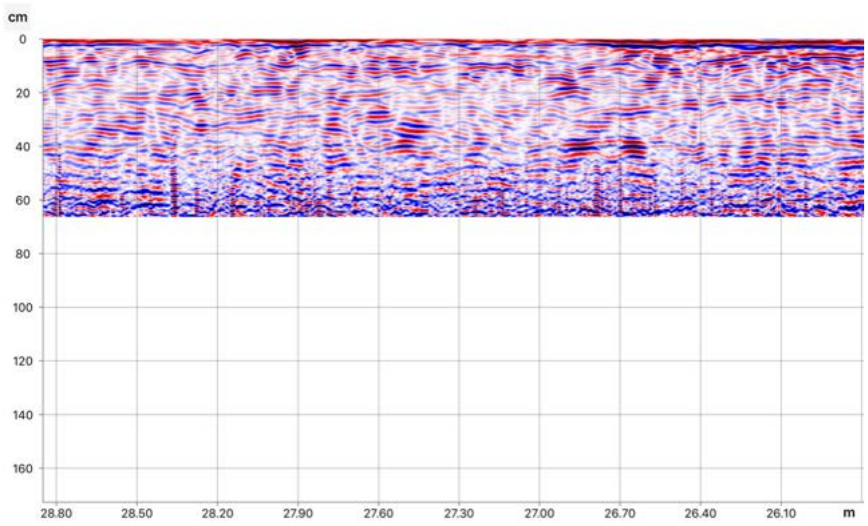

Figure 10. A portion of G1 transect radargram

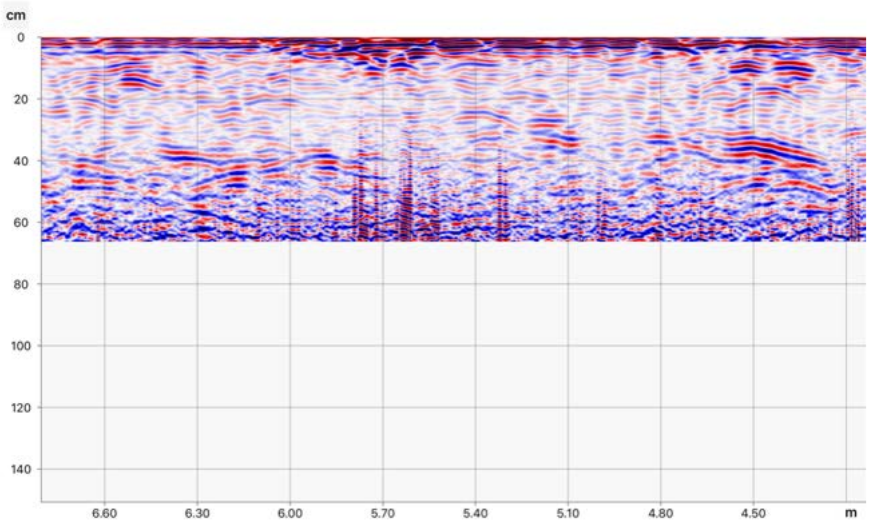

Interpretation of compaction:

GPR signals produce an image that represents structural differences within a medium. Thus, strong reflections found in the transect radargrams may be suggestive of soil compaction by

[12] This will be further discussed in Soil Analysis.

a change in structural properties within the soil. Figures 11 and 12 demonstrate strong reflections suggesting compaction that are substantiated by the penetrometer results at that location.

Figure 11. Radargram showing compaction in G1

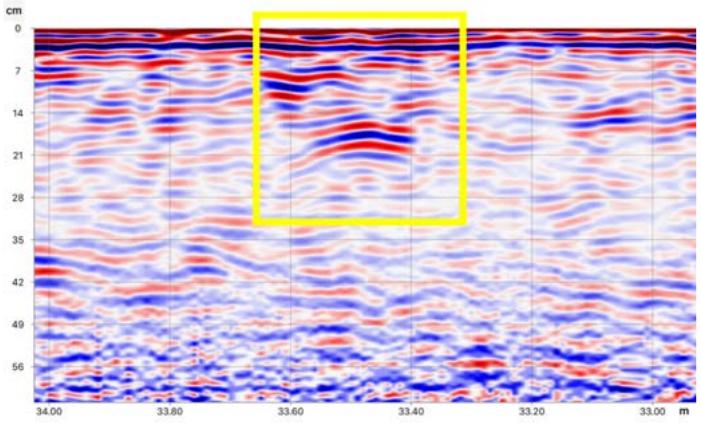

Figure 12. Radargram showing compaction in G6

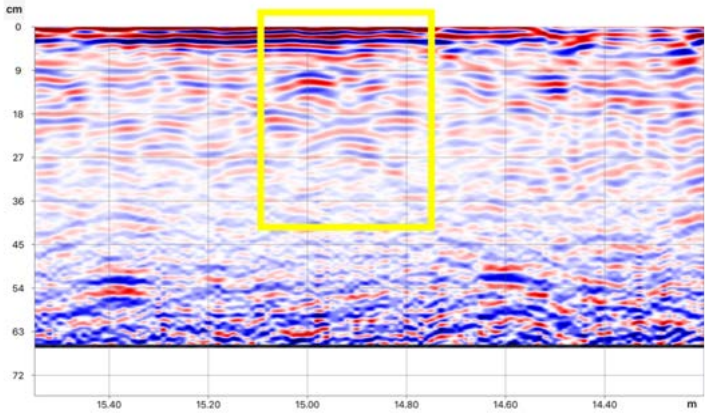

While the overall level of soil compaction from the penetrometer readings at site A were minimal, transect A6 displayed unusually higher readings when compared to the five adjacent transects. Six readings, taken within 9 meters, showed high levels of compaction (4 out of 6 readings with an average cone index ≥250 psi). It was observed that this segment of the transect had visible traces of one or more tractor passes which may have influenced the abnormal level of compaction. Figure 13 illustrates the segment of G6 in which the penetrometer recorded soil compaction. This also provides a clear example of signal attenuation beginning at ~32 cm.

Figure 13. Compaction and signal attenuation in G6

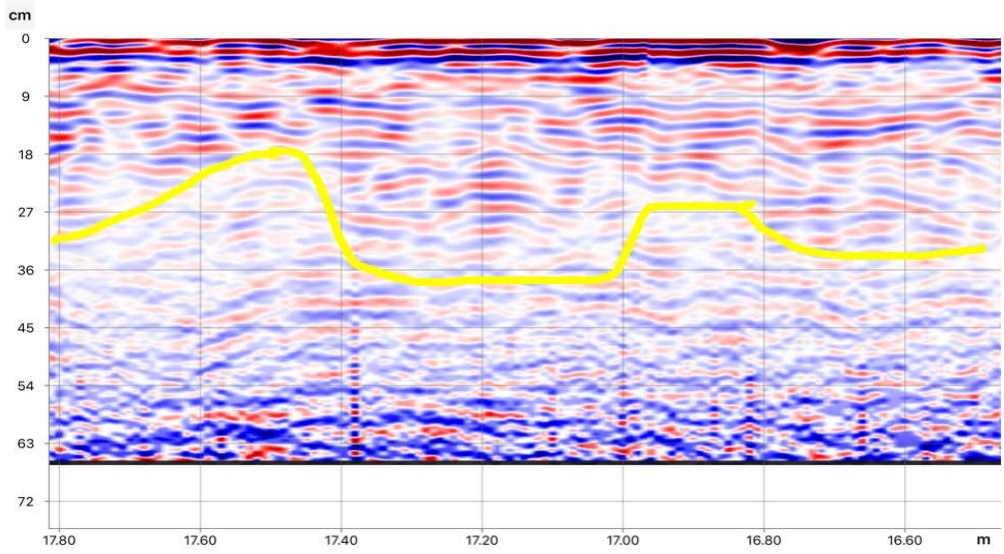

Figure 14. Soil compaction, rock, and pipe in G6

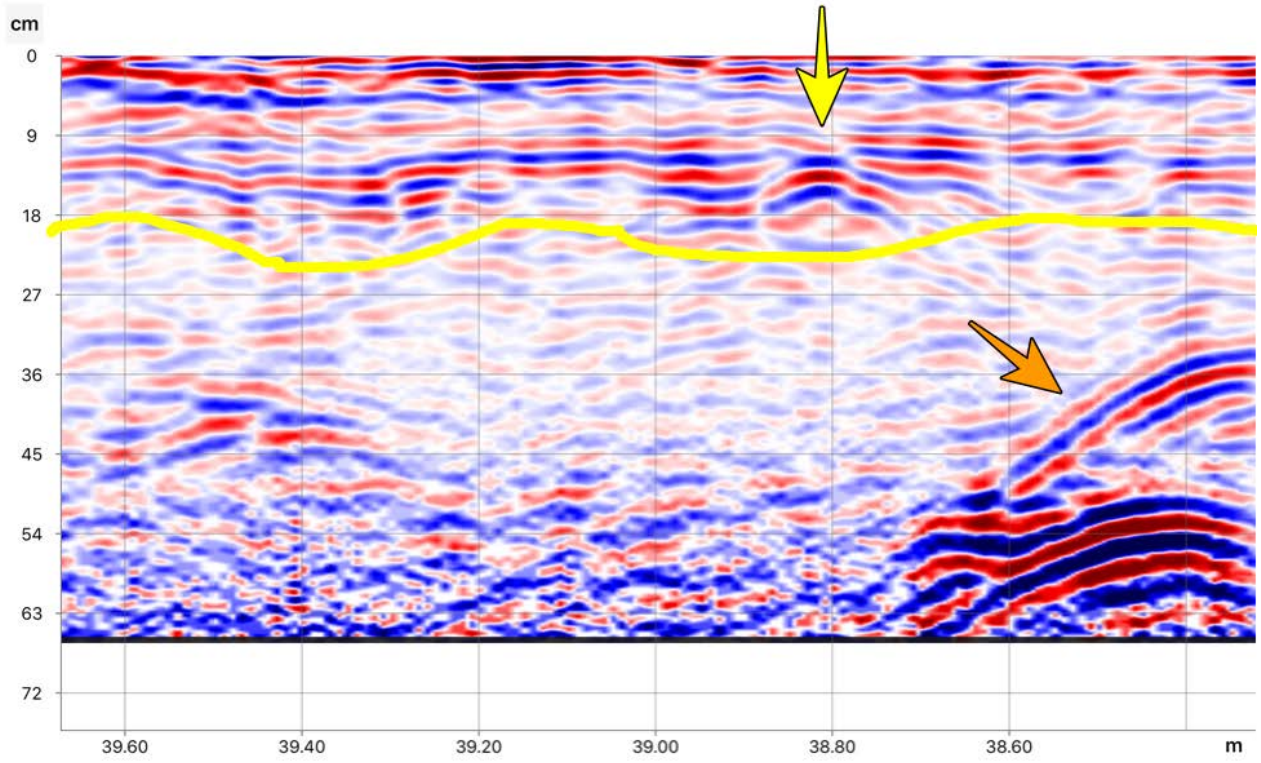

Figure 14 illustrates the end of transect G6 which is located adjacent to a grouping of trees that was cultivated sometime between 2011 and 2013 according to information gleaned from Google Earth Pro. The GPR signals show a change of structure in this area, likely indicating soil compaction substantiated by high penetrometer readings. This compaction could be related to the cultivation and management of the trees as heavy machinery would have moved along the perimeter of the block in the early stages of cultivation. The yellow arrow provides an example indicating the location of a possible object, such as a rock, by the distinguishing hyperbola. The orange arrow indicates the detection of a pipe located perpendicular to the transect which was also detected in four other radargrams at the northern end of the site.

Areas where the penetrometer found little compaction were compared to the GPR signals in the radargrams. These areas were consistently found to have weaker GPR reflections when compared to the GPR signals in areas where the penetrometer readings indicated high compaction. An example of where the penetrometer indicated little compaction can be visualized in Figure 15.

Figure 15. Example of little compaction in A3

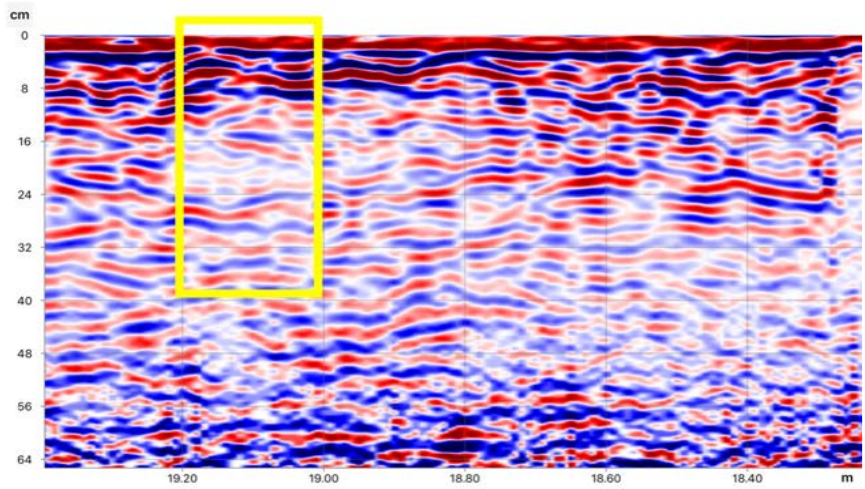

Figure 16. GPR error

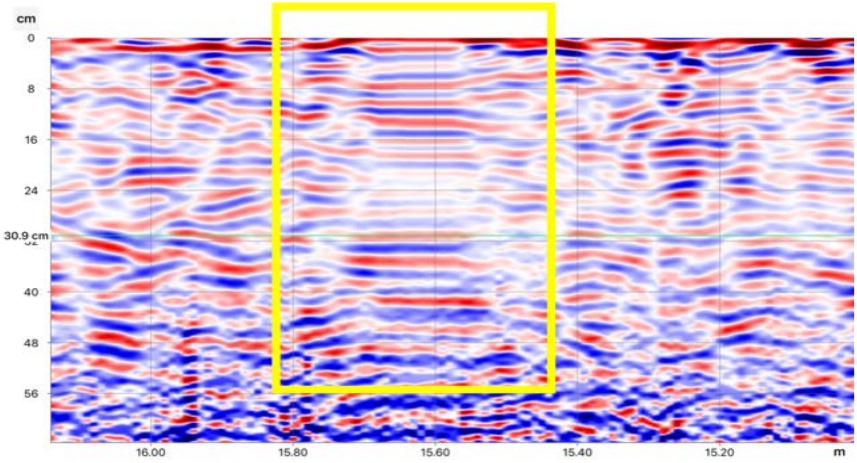

Due to issues regarding the design of the GPR model[13], errors in the reading of GPR signals were frequent as a result of the difficulty in rolling the equipment across the varied terrain. The equipment wheels frequently stalled triggering staggered transmission and reception of GPR signals. As a result, there were inaccurate measurements of distance present on the radargrams. To mitigate these inaccuracies, the radargrams were scaled during processing. This provides a limitation as it introduced some level of inaccuracy when comparing the variables. An example of this type of error is visualized in Figure 16.

Determining depth to compaction:

Depth to compaction was estimated by interpreting radargrams. This was necessary in to provide a full dataset regarding the field measurements for statistical analysis. Depth to compaction was estimated at the locations where core samples and penetrometer readings were

[13] Although the mechanism of GPR remain constant among varying makes and models, the model used for this study was designed for rolling over cement.

taken. At these locations, the radargrams were observed and areas of moderate to intense reflections were interpreted as soil compaction. The corresponding depth was provided by the y-axis and recorded. The limitation of this strategy is from human error during interpretation. Additionally, the GPR may not always accurately detect soil compaction as signals may be prematurely attenuated in the presence of material with high dielectric constants.

Soil analysis

Although differences were expected, the soil samples showed little variability in soil physical properties and organic matter content between the sites. As a result of the high incidence of cone index readings > 300 psi in the grass site, the average dry bulk density was expected to be larger than the agriculture site, however, dry bulk densities from both sites were virtually the same at both depths sampled (see Table 2). Similarly, after processing samples using the LOI method, percent soil organic matter (SOM) and carbon stocks did not reveal substantial differences between the sites (see Table 2).

One possible explanation for the uniformity between sites is the recent change in land cover and management. As detailed in the section site history, the agriculture site was transitioned to a cultivated field in 2016. The agriculture field is not intensively managed for production, but rather used for intermittent research studies by students at the University. This implies less frequent mechanical manipulation and amending of the soil. Thus, it can be inferred that the physical soil characteristics and organic matter content between both sites, although they are currently under varying land uses, are very similar. However, interestingly, the upper horizon of the agriculture field comprised a slightly higher carbon stock when compared to the lower depth sampled at that site and both depths in the grass site. This may be explained by an organic amendment applied to the surface of the site not long before* field measurements were taken.

Table 2. Physical soil properties and organic matter content at site A and G[14]

Site	***Depth***	***Gravimetric soil water content* (g g^{-1})***	***Bulk density* (g cm^{-3})***	***Carbon stock* (g)***	***% SOM (LOI350)****
Agriculture	10	0.28 ± 0.03	1.09 ± 0.09	3.06 ± 0.18	7.69 ± 0.66
	20	0.27 ± 0.04	1.08 ± 0.09	2.90 ± 0.32	7.60 ± 0.64
Grass	10	0.27 ± 0.03	1.05 ± 0.09	2.96 ± 0.55	7.76 ± 0.83
	20	0.26 ± 0.04	1.04 ± 0.07	2.71 ± 0.35	7.21 ± 0.77

*Values denote mean ± 1SD.

[14] Refer to Appendix D for raw data.

Principal component analysis

The principal component analysis provided a biplot (see Figure 17) distinguishing the agriculture and grass site by variables measured and allowed for exploratory analysis of the dataset. The PCA accounted for 69 percent of the variation within the data, as can be identified by combining the percent variation present on both axes. This is a relatively weak variation and does not allow for an accurate representation of the data; however, the two principal components with the largest variation may be used to identify clusters and patterns in the data. Most notably, the biplot demonstrates correlations between moisture and carbon stock at both depths; however, the analysis shows a weak relationship illustrated by the loadings. Additionally, the biplot illustrates that the agriculture field has higher moisture and carbon stock than the grass site, although these differences are minimal. There is no correlation between depth to compaction and soil moisture, suggesting that these two factors have little effect on each other. Lastly, when comparing the clusters of both sites, far more variability is present in the agriculture site.

Figure 17. PCA of field measurement dataset

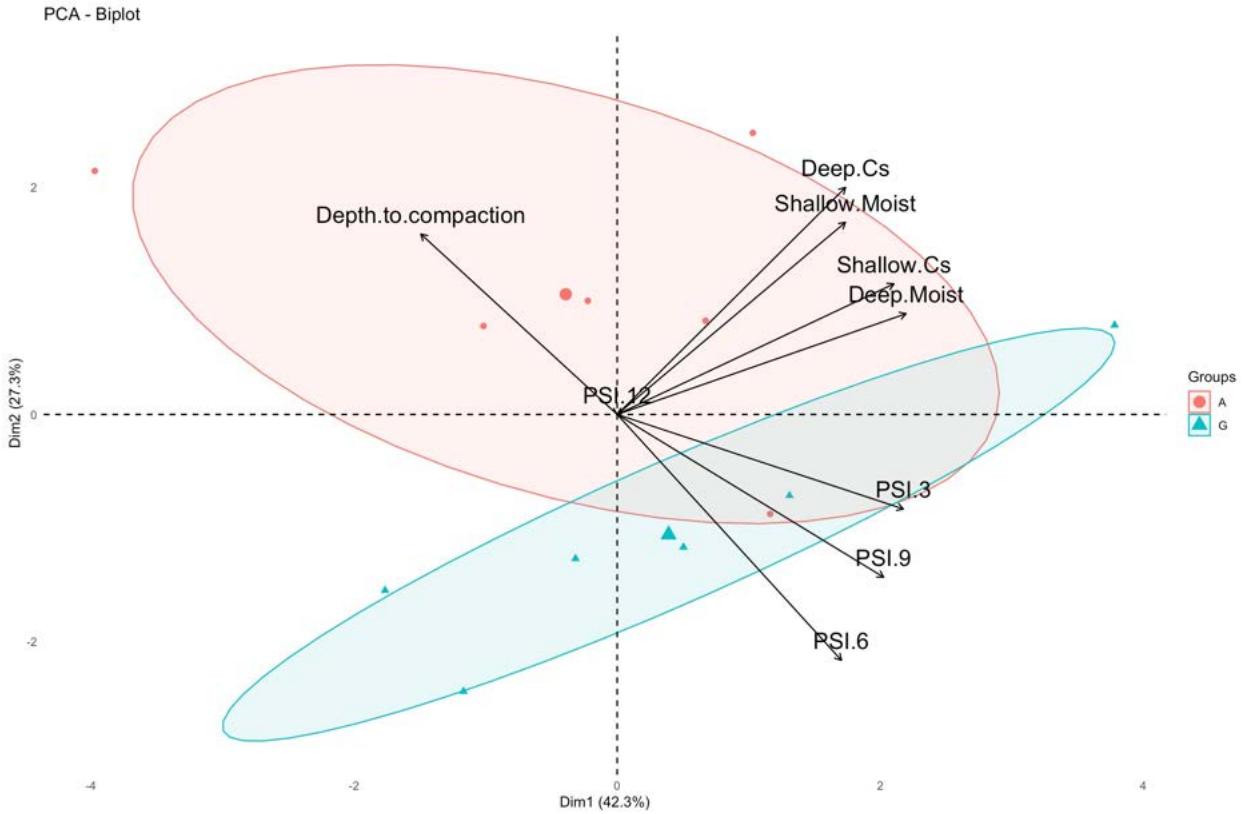

Scope and Limitations

Although this report emphasized the Fraser-Nooksack Lowlands, it should be noted that this region contains a large variety of soil types and biophysical contexts in which GPR scans may not be appropriate. The results and conclusions from the field study within this report are therefore limited to sites that are relatively level, have low organic matter and moisture, and are sandy loam soil in texture.

Field study limitations

The overall spatial homogeneity of the sites studied at Totem field provided a limitation in that differences between the sites were often undiscernible leading to difficultly comparing the GPR data. Future research would benefit from choosing contrasting sites in order to compare reflection coefficients and signal velocity in the radargrams and to further explore differences in soil properties through penetrometer resistance and soil analysis with GPR results.

GPR technology is limited by the inability to distinguish objects from one another. The technology provides a radargram which must be interpreted, leaving the possibility for human error compounded by possible lack of experience. Significant time is required to learn and understand the technology, how to operate the device, and how to interpret the findings. This may be a significant limitation for land managers considering GPR for soil compaction assessments.

Recommendations

Ground-penetrating radar

- Costs associated with GPR equipment might be a significant limitation for land managers. A simple GPR system is quoted to cost upwards of USD 15,000. The rental fee associated with the equipment used in this study was CAD 450/week from Hoskin Scientific LTD. However, as mentioned previously, there is a steep learning curve for individuals unaccustomed to this technology. Alternatively, local companies advertise GPR surveying and interpretation at a daily cost between CAD 1000 and 2000, depending on the project size. It is recommended that more studies assessing GPR and soil compaction in varying soil types with the Fraser-Nooksack Lowlands be conducted before land managers invest in this technology.
- As discussed, the GPR model employed in the field study was not appropriate for soil assessment in agri-food systems. It is recommended that future research utilize a GPR with portable equipment that is suitable for moving through bare soil, cultivated fields, forested areas, and grass. Additionally, the use of a GPS device would facilitate tracking GPR scans and distances.

- Through the literature review, it was discovered that a GPR assessment would be not useful in saturated and/or clayey soils as elevated signal attenuation from the high dielectric constants will result in poor resolution radargrams. It is therefore recommended that future GPR assessments occur in predominantly loamy soils, and that assessments be avoided during the winter rainy season in the Fraser-Nooksack Lowlands.

Future research

- There is potential for future MLWS students to use this study as a beginning point for a comprehensive analysis of spatial variability soil compaction and the implication for infiltration and groundwater recharge in agri-food systems within the Fraser-Nooksack Lowlands. The literature review and preliminary GPR calibration conducted within this project can function as a starting-off point for a study in which GPR equipment can be utilized for taking field measurements and analysis.

Concluding Remarks

The relationship of soil compaction to the hydrological cycle is an important consideration from the perspective of land managers. Although the interconnectedness of physical soil properties and the hydrological cycle may be difficult to discern, it is an imperative connection that maintains agricultural production. The ability of water to infiltrate soil is necessary for both soil water storage and its percolation to recharge groundwater and aquifers. Producers may rely heavily on both of these water sources to meet production demands. It is therefore necessary to develop and execute an accessible and efficient strategy for assessing soil compaction and spatial variability within an agri-food system. This study aimed to understand how GPR technology may be used to fulfil this need in the Fraser-Nooksack Lowlands. A qualitative field study was conducted and found that GPR technology has the potential to be a practical assessment tool. Further research is recommended to provide additional information on the usefulness of this technology in varying agri-food systems within the Fraser-Nooksack Lowlands.

References

Abdi, H., & Williams, L. J. (2010). Principal component analysis. *Wiley Interdisciplinary Reviews: Computational Statistics*, *2*(4), 433–459. https://doi.org/10.1002/wics.101

Akinsunmade, A., Tomecka-Suchoń, S., & Pysz, P. (2019). Correlation between agrotechnical properties of selected soil types and corresponding GPR response. *Acta Geophysica*, *67*(6), 1913–1919. https://doi.org/10.1007/s11600-019-00349-4

Alaoui, A., Rogger, M., Peth, S., & Blöschl, G. (2018). Does soil compaction increase floods? A review. *Journal of Hydrology*, *557*, 631–642. https://doi.org/10.1016/j.jhydrol.2017.12.052

Balugani, E., Lubczynski, M. W., Reyes-Acosta, L., van der Tol, C., Francés, A. P., & Metselaar, K. (2017). Groundwater and unsaturated zone evaporation and transpiration in a semi-arid open woodland. *Journal of Hydrology*, *547*, 54–66. https://doi.org/10.1016/j.jhydrol.2017.01.042

Batey, T. (2009). Soil compaction and soil management – a review. *Soil Use and Management*, *25*(4), 335–345. https://doi.org/10.1111/j.1475-2743.2009.00236.x

Bogunovic, I., Pereira, P., Kisic, I., Sajko, K., & Sraka, M. (2018). Tillage management impacts on soil compaction, erosion and crop yield in Stagnosols (Croatia). *Catena*, *160*(October 2017), 376–384. https://doi.org/10.1016/j.catena.2017.10.009

Brady, N. C., & Weil, R. R. (2010). *Elements of the nature and properties of soils* (3rd ed.). Pearson.

Buckley, P. H., Belec, J., & Levy, J. (2015). Environmental resource management in borderlands: Evolution from competing interests to common aversions. *International Journal of Environmental Research and Public Health*, *12*(7), 7541–7557. https://doi.org/10.3390/ijerph120707541

Carrick Utsi, E. (2017). Fundamentals of GPR Operation. In *Ground Penetrating Radar* (pp. 1–11). https://doi.org/10.1016/b978-0-08-102216-0.00001-1

Duiker, S. W. (2002). *Diagnosing Soil Compaction Using a Penetrometer (Soil Compaction Tester)*. https://extension.psu.edu/diagnosing-soil-compaction-using-a-penetrometer-soil-compaction-tester

Enivonmental Protection Agency. (n.d.). *Ground-penetrating radar*. https://archive.epa.gov/esd/archive-geophysics/web/html/ground-penetrating_radar.html

Freeland, R. S., Sorochan, J. C., Goddard, M. J., & Mcelroy, J. S. (2008). *Using ground-penetating radar to evaluate soil compaction of athletic turfgrass fields*. *24*(4), 509–514.

Gifford, R. M., & Roderick, M. (2003). Soil carbon stocks and bulk density : spatial or cumulative mass coordinates as a basis of expression ? *Global Change Biology*, *9*, 1507–1514. https://doi.org/10.1046/j.1529-8817.2003.00677.x

Healy, R. W., & Scanlon, B. R. (2010). Groundwater recharge. In *Estimating Groundwater Recharge* (pp. 1–14). Cambridge University Press. https://doi.org/10.1017/CBO9780511780745.002

Hemmat, A., & Adamchuk, V. I. (2008). Sensor systems for measuring soil compaction: Review and analysis. *Computers and Electronics in Agriculture*, *63*(2), 89–103. https://doi.org/10.1016/j.compag.2008.03.001

Hoogsteen, M. J. J., Lantinga, E. A., Bakker, E. J., Groot, J. C. J., & Tittonell, P. A. (2015). Estimating soil organic carbon through loss on ignition: Effects of ignition conditions and structural water loss. *European Journal of Soil Science*, *66*(2), 320–328. https://doi.org/10.1111/ejss.12224

Jensen, J. L., Christensen, B. T., Schjønning, P., Watts, C. W., & Munkholm, L. J. (2018). Converting loss-on-ignition to organic carbon content in arable topsoil: pitfalls and proposed procedure. *European Journal of Soil Science*, *69*(4), 604–612. https://doi.org/10.1111/ejss.12558

Kovanen, D., & Slaymaker, O. (2015). The paraglacial geomorphology of the Fraser Lowland, southwest British Columbia and northwest Washington. *Geomorphology*, *232*, 78–93. https://doi.org/10.1016/j.geomorph.2014.12.021

Murdock, L., Gray, T., Higgins, F., & Wells, K. (1993). *Soil Compaction in Kentucky*. 1–4.

Nawaz, M. F., Bourrié, G., & Trolard, F. (2013). Soil compaction impact and modelling. A review. *Agronomy for Sustainable Development*, *33*(2), 291–309. https://doi.org/10.1007/s13593-011-0071-8

Nelson, D., & Sommers, L. (1996). Chemical Methods Soil Science Society of America Book Series. In J. M. Bigham (Ed.), *Soil Science Society of America and American Society of Agronomy. Methods of Soil Analysis. Part 3.* (Issue Chemical Methods-SSSA Book Series no. 5, pp. 1001-1006.). https://www.waterboards.ca.gov/waterrights/water_issues/programs/bay_delta/california_waterfix/exhibits/docs/Islands/II_41.pdf

Rast, M., Johannessen, J., & Mauser, W. (2014). Review of Understanding of Earth's Hydrological Cycle: Observations, Theory and Modelling. *Surveys in Geophysics*, *35*(3), 491–513. https://doi.org/10.1007/s10712-014-9279-x

Sood, A., Prathapar, S. A., & Smakhtin, V. (2014). Green and Blue Water. *Key Concepts in Water Resource Management: A Review and Critical Evaluation*, 91–102. https://doi.org/10.4324/9781315884394

Spoor, G. (2006). Alleviation of soil compaction: Requirements, equipment and techniques. *Soil Use and Management*, *22*(2), 113–122. https://doi.org/10.1111/j.1475-2743.2006.00015.x

Trenberth, K. E. (2011). Changes in precipitation with climate change. *Climate Research*, *47*(1–2), 123–138. https://doi.org/10.3354/cr00953

Wang, P., Hu, Z., Zhao, Y., & Li, X. (2016). Experimental study of soil compaction effects on GPR signals. *Journal of Applied Geophysics*, *126*, 128–137. https://doi.org/10.1016/j.jappgeo.2016.01.019

Acknowledgements

First and foremost, the author would like to extend sincere gratitude and thanks to Dr. Les Lavkulich and Julie Wilson for their mentorship and encouragement throughout the Master of Land and Water Systems (MLWS) program. The author would like to thank Lewis Fausak for his significant contributions in both collecting field measurements and data processing; Ian Josephson for his expert assistance in soil sampling and unconditional encouragement; Dr. Heather Mackay for her helpful feedback; and MLWS friends for their emotional and academic support as well as their friendship throughout this process.

Appendices

Appendix A

Figure 18. Climate normals from 1981 to 2010 at Vancouver International Airport Station. Source: Environment Canada

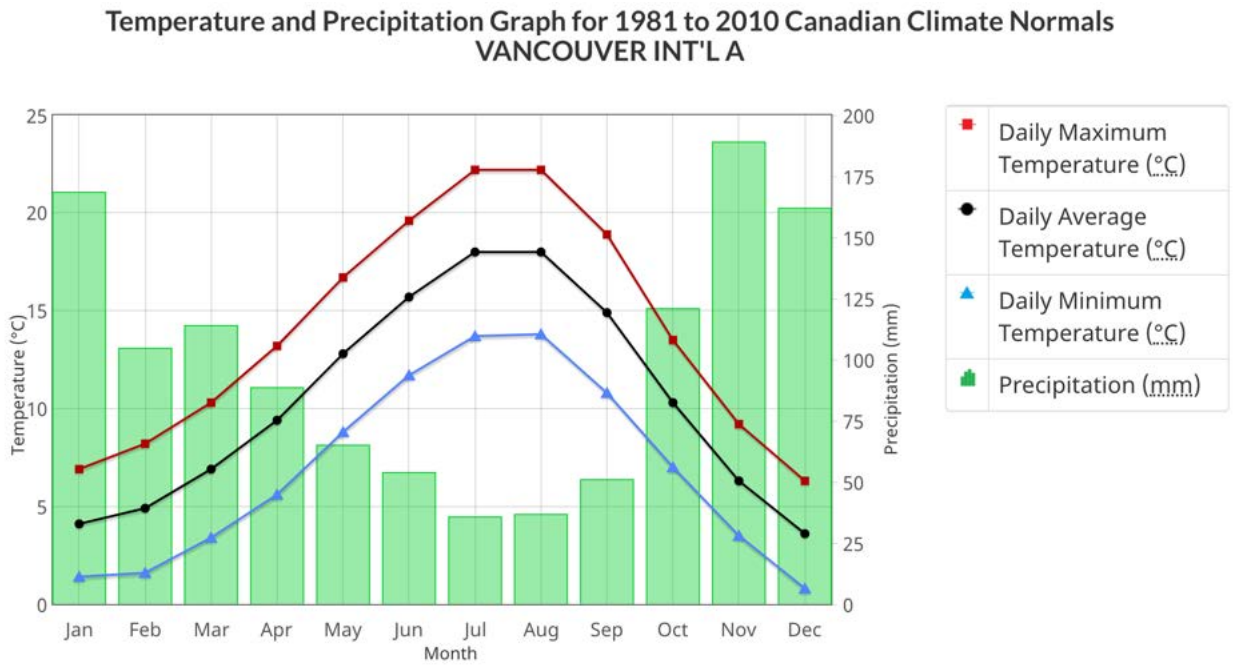

Table 3. Electromagnetic properties of earth materials. Source: (Environmental Protection Agency, n.d.)

Material	E	Condutivity	Velocity, (m/ns)	Attenuation, (dB/m)
Air	1	0	0.3	0
Distilled Water	80	0.001	0.033	0.002
Frest Water	80	0.5	0.033	0.1
Sea Water	80	3,000	0.01	1,000
Dry Sand	3-5	0.01	0.15	0.01
Wet Sand	20-30	0.1-1	0.06	0.03-0.3
Limestone	4-8	0.5-2	0.12	0.4-1
Shales	5-15	1-100	0.09	1-100
Silts	5-30	1-100	0.07	1-100
Clays	5-40	2-1,000	0.06	1-300
Granite	4-6	0.01-1	0.13	0.01-1
Dry Salt	5-6	0.01-1	0.13	0.01-1
Ice	3-4	0.01	0.16	0.01
Metal				

Appendix B

Figure 19. Site map with transects. This map illustrates an approximation of site A (red) and site G (yellow) with 6 x 42 m transects per site. Courtesy of Google Earth Pro.

Appendix C

Table 4. Penetrometer readings for site G.

Grass site	Cone index				
	1	2	3	4	Location (m)
G1-1	50	50	300	>300	3
G1-2	10	275	>300	>300	7
G1-3	100	300	>300	>300	9
G1-4	75	250	300	>300	20
G1-5	100	225	300	>300	27
G1-6	100	300	>300	>300	35
G1-7	100	275	300	>300	37
G1-8	75	200	300	>300	39
G2-1	200	250	>300	>300	1
G2-2	175	200	>300	>300	3
G2-3	175	>300	>300	>300	8
G2-4	100	250	>300	>300	11
G2-5	75	300	>300	>300	14
G2-6	50	200	>300	>300	25
G2-7	75	190	>300	>300	27
G2-8	100	200	>300	>300	30
G3-1	175	260	>300	>300	15
G3-2	125	300	>300	>300	21
G3-3	75	175	275	>300	23
G3-4	75	225	>300	>300	28
G3-5	75	200	>300	>300	29
G3-6	75	230	>300	>300	30
G3-7	75	200	>300	>300	36
G3-8	125	250	>300	>300	38
G4-1	200	>300	>300	>300	3
G4-2	100	>300	>300	>300	12
G4-3	200	>300	>300	>300	17
G4-4	100	300	>300	>300	18
G4-5	100	275	>300	>300	21
G4-6	125	>300	>300	>300	25
G4-7	190	>300	>300	>300	40
G4-8	190	260	>300	>300	41
G5-1	>300	>300	>300	>300	2
G5-2	>300	>300	>300	>300	5

G5-3	300	>300	>300	>300	14
G5-4	260	>300	>300	>300	15
G5-5	>300	>300	>300	>300	18
G5-6	>300	>300	>300	>300	28
G5-7	>300	>300	>300	>300	29
G5-8	75	190	275	>300	42
G6-1	200	>300	>300	>300	16
G6-2	125	250	275	>300	18
G6-3	225	300	>300	>300	19
G6-4	175	>300	>300	>300	20
G6-5	200	>300	>300	>300	25
G6-6	175	>300	>300	>300	33
G6-7	275	>300	>300	>300	37
G6-8	125	>300	>300	>300	42

Table 5. Penetrometer readings for site A.

Agriculture site	**Cone index**				
	1	**2**	**3**	**4**	**Location (m)**
A1-1	125	140	250	>300	0
A1-2	0	50	100	>300	5
A1-3	100	150	250	>300	9
A1-4	100	150	275	>300	15
A1-5	75	100	100	>300	21
A1-6	25	25	250	>300	31
A1-7	0	0	200	>300	34
A1-8	125	200	250	>300	37
A2-1	100	100	>300	>300	3
A2-2	100	>300	>300	>300	4
A2-3	125	150	>300	>300	13
A2-4	0	125	150	>300	15
A2-5	100	200	200	>300	17
A2-6	25	100	100	>300	23
A2-7	150	290	>300	>300	36
A2-8	200	250	>300	>300	40
A3-1	125	150	275	250	0
A3-2	125	150	>300	>300	3
A3-3	0	50	100	>300	6
A3-4	0	200	175	>300	14

A3-5	50	100	150	>300	17
A3-6	0	25	25	>300	28
A3-7	75	110	100	>300	32
A3-8	25	75	75	>300	34
A4-1	150	125	>300	>300	5
A4-2	125	175	225	>300	6
A4-3	150	150	>300	>300	17
A4-4	175	175	275	>300	18
A4-5	150	240	275	>300	34
A4-6	40	50	75	>300	37
A4-7	25	25	>300	>300	38
A4-8	125	150	150	>300	41
A5-1	50	100	>300	>300	1
A5-2	75	125	>300	>300	2
A5-3	0	25	250	>300	4
A5-4	100	175	275	>300	9
A5-5	75	150	150	>300	13
A5-6	100	250	>300	>300	31
A5-7	200	200	250	>300	36
A5-8	50	200	200	>300	41
A6-1	150	>300	>300	>300	3
A6-2	50	100	>300	>300	7
A6-3	75	150	>300	>300	17
A6-4	150	>300	>300	>300	18
A6-5	100	225	>300	>300	19
A6-6	125	>300	>300	>300	20
A6-7	>300	>300	>300	>300	22
A6-8	100	>300	>300	>300	26

Appendix D

Table 6. Site G soil moisture and bulk density measurements

Grass site	*Location*	*θg shallow*	*θg deep*	*Pb shallow*	*Pb deep*
G1-2	7	0.29	0.21	1.01	1.1
G1-4	20	0.26	0.28	0.96	1.03
G1-6	35	0.27	0.28	1.12	1
G2-1	1	0.23	0.22	1.16	1.08
G2-3	8	0.25	0.24	1.08	1.05
G2-5	14	0.31	0.33	1.22	1.06
G3-1	15	0.30	0.26	1.00	1.06
G3-2	21	0.30	0.26	1.05	1.02
G3-7	36	0.26	0.26	0.93	0.88
G4-2	12	0.28	0.26	1.10	1.08
G4-3	17	0.30	0.28	0.97	1.09
G4-5	21	0.29	0.28	1.00	1.19
G5-2	5	0.20	0.19	1.07	1.12
G5-6	28	0.29	0.32	1.23	1.06
G5-8	42	0.25	0.22	0.98	0.99
G6-3	19	0.31	0.28	1.08	1.03
G6-6	33	0.26	0.30	0.97	0.96
G6-7	37	0.25	0.25	1.04	0.99

Table 7. Site A soil moisture and bulk density measurements

Agriculture site	*Location*	*θg shallow*	*θg deep*	*Pb shallow*	*Pb deep*
A1-2	5	0.25	0.29	0.92	1.07
A1-3	9	0.30	0.27	1.02	0.88
A1-4	15	0.27	0.27	1.11	1.01
A2-3	13	0.29	0.30	1.11	1.08
A2-6	23	0.24	0.26	1.27	1.21
A2-7	36	0.25	0.16	1.11	1.16
A3-2	3	0.34	0.36	1.15	1.18
A3-6	28	0.25	0.25	1.16	1.05
A3-8	34	0.25	0.24	1.23	1.17
A4-1	5	0.33	0.32	1.01	1.05
A4-4	18	0.28	0.28	1.05	1.05
A4-5	24	0.28	0.25	1.10	1.22
A5-1	1	0.32	0.32	0.93	1
A5-7	36	0.25	0.26	1.15	1.02
A5-8	41	0.22	0.23	1.02	1.05
A6-4	18	0.28	0.27	1.06	1.08
A6-6	20	0.29	0.27	1.06	1.15
A6-8	26	0.27	0.31	1.15	0.94

Appendix E

Each radargram represents the full length of a transect. The arrows denote where penetrometer resistance readings were taken. Red arrows represent high compaction readings, yellow represents moderate compaction and green low compaction. The yellow dotted line superimposed on each radargram demonstrates the minimum and maximum depth in which penetrometer readings were taken. The X denotes where a core sample was taken at two depths (~10 cm and ~20 cm).

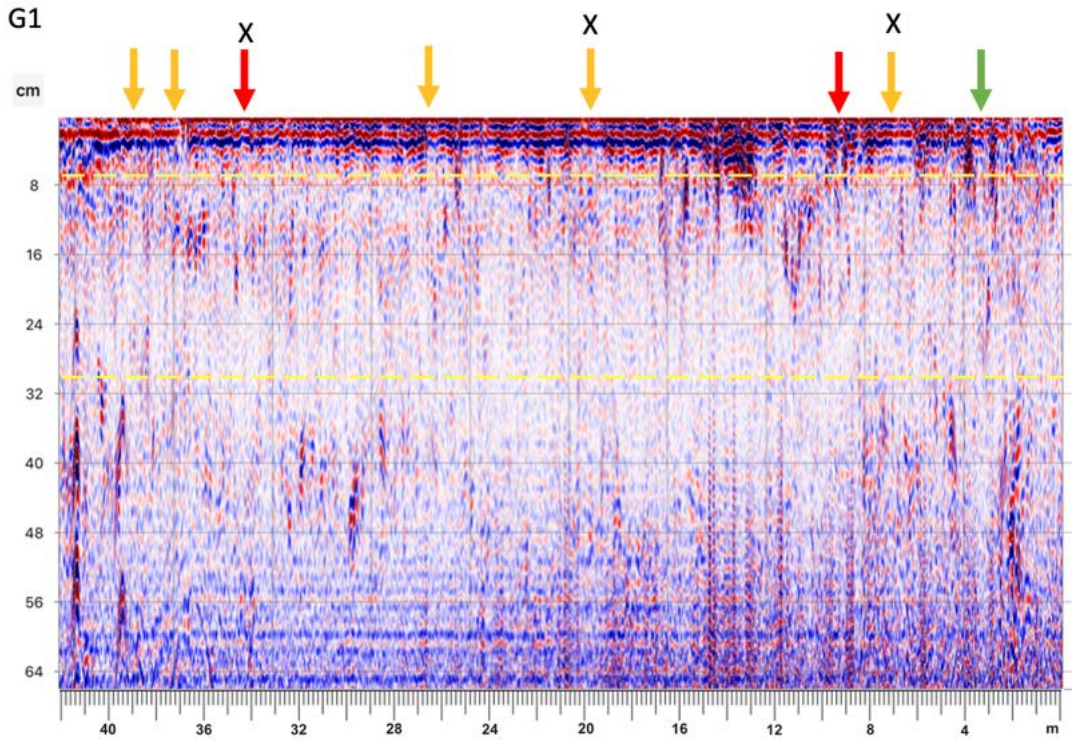

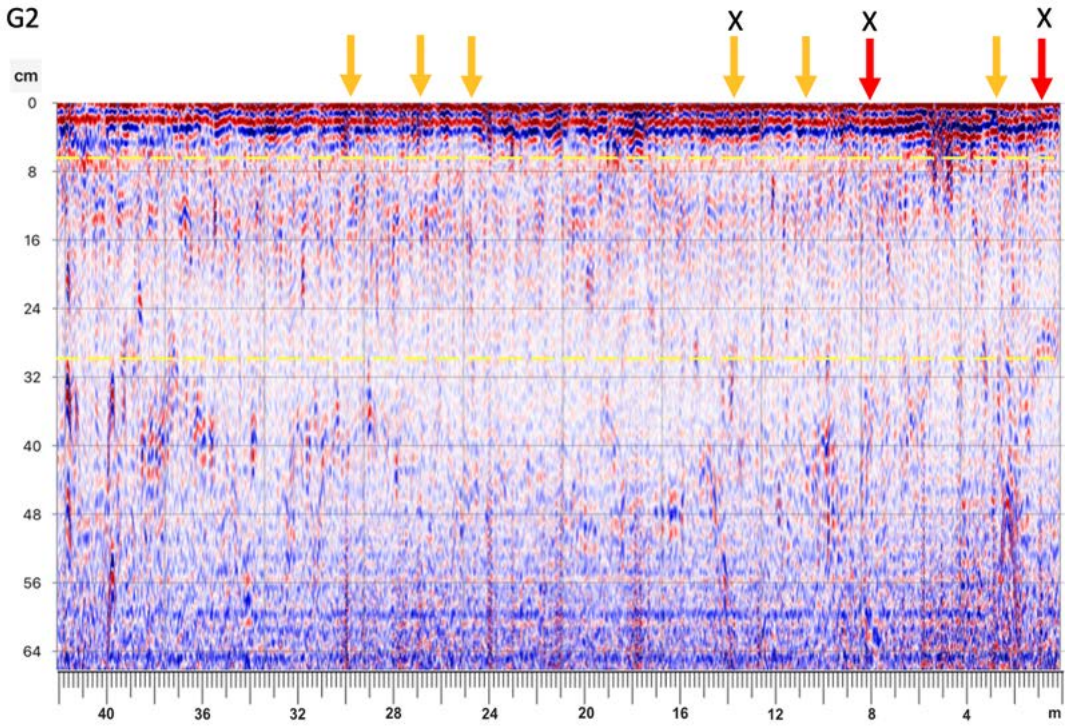
G2
cm
0
8
16
24
32
40
48
56
64
X
X
X
40
36
32
28
24
20
16
12
8
4
m

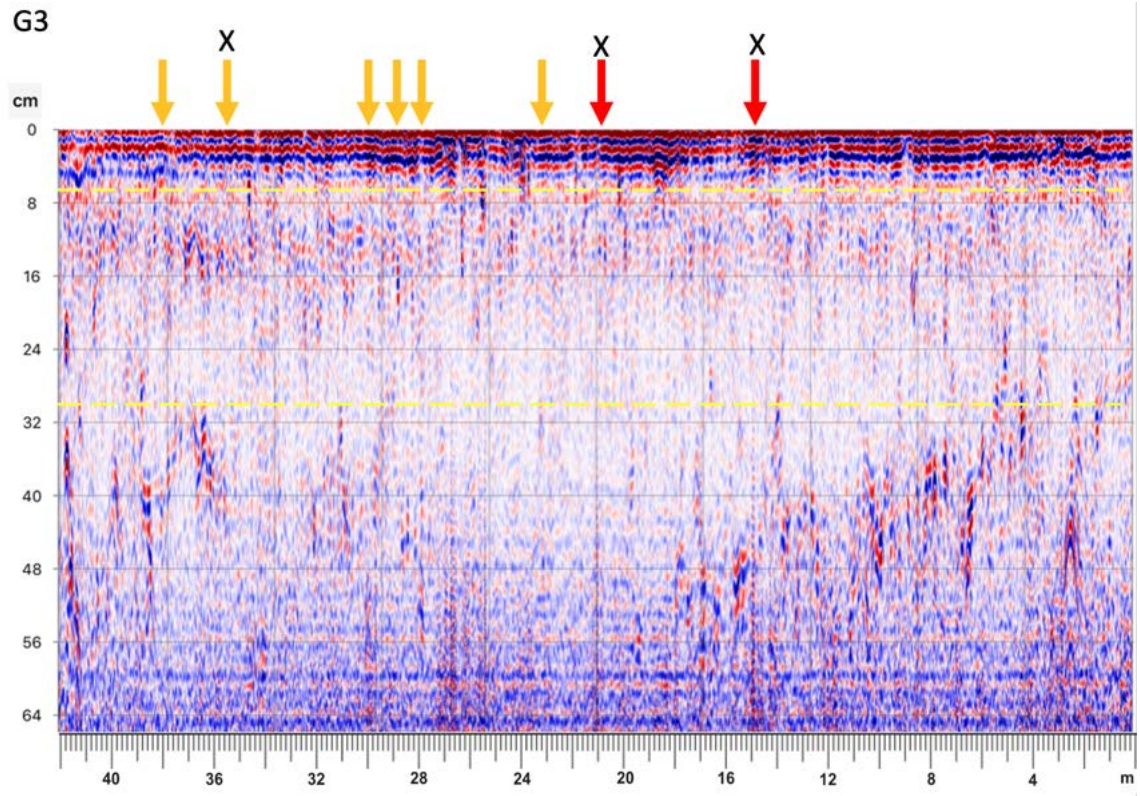
G3
cm
0
8
16
24
32
40
48
56
64
X
X
X
40
36
32
28
24
20
16
12
8
4
m

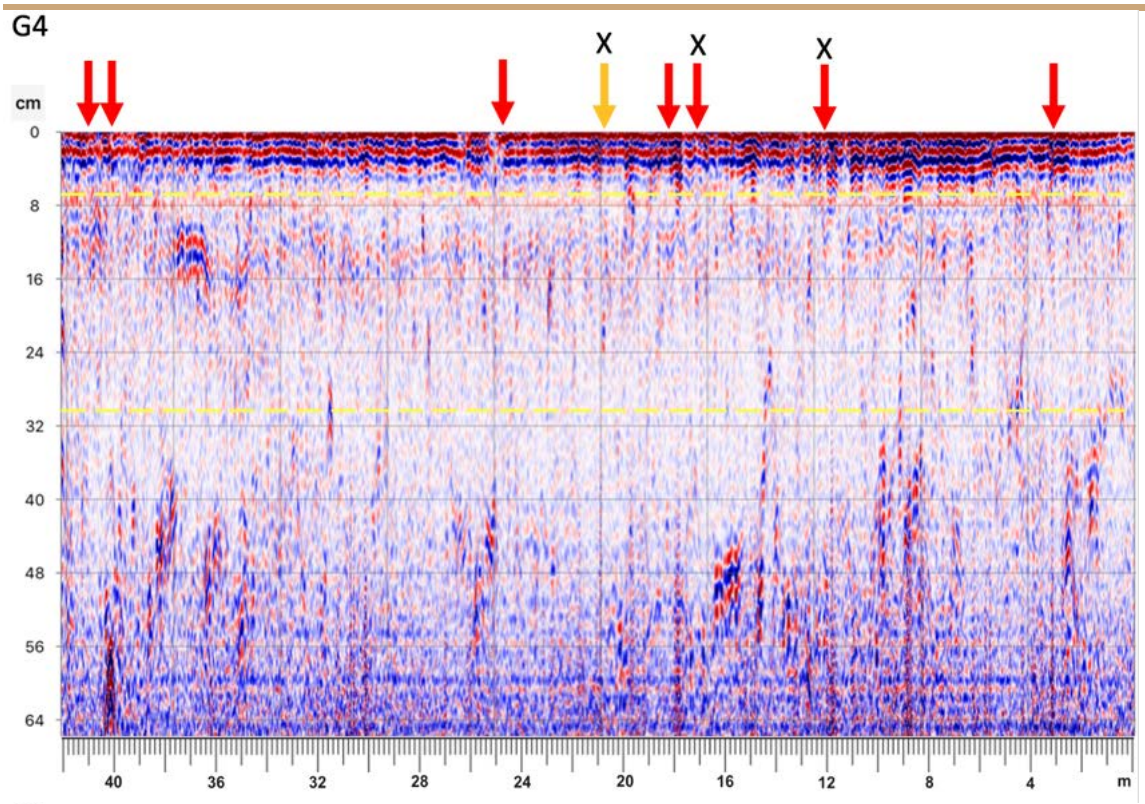
G4
X
X
X
cm
0
8
16
24
32
40
48
56
64
40
36
32
28
24
20
16
12
8
4
m

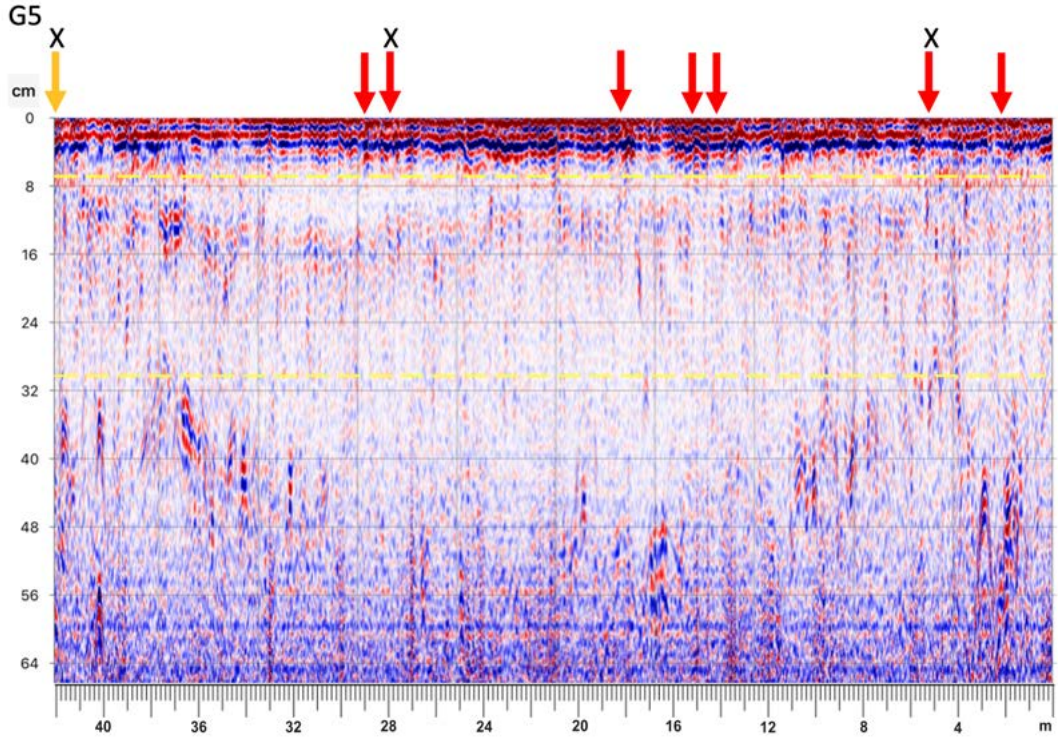
G5
X
X
X
cm
0
8
16
24
32
40
48
56
64
40
36
32
28
24
20
16
12
8
4
m

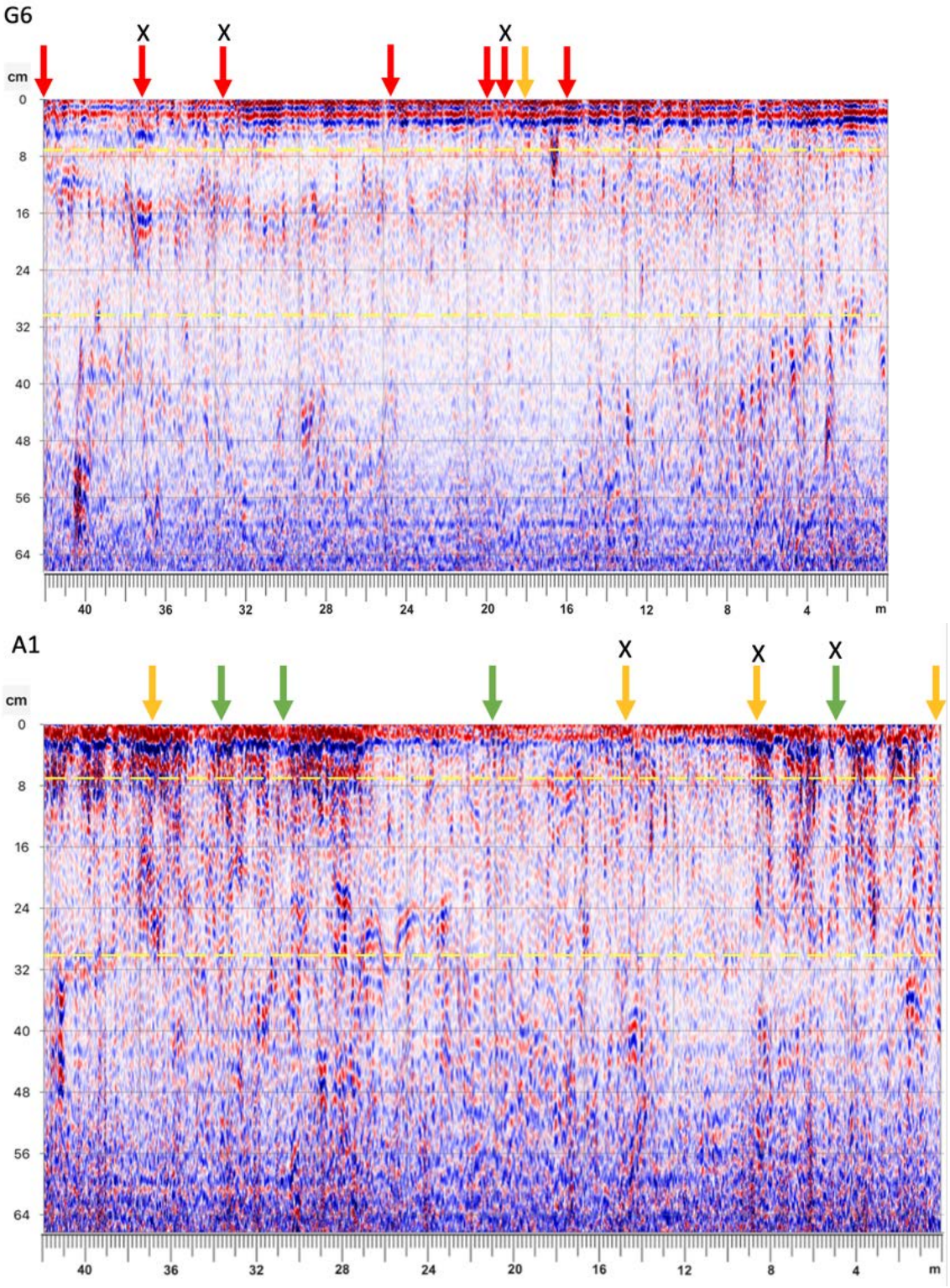
G6
X
X
X
cm
0
8
16
24
32
40
48
56
64
40
36
32
28
24
20
16
12
8
4
m
A1
X
X
X
cm
0
8
16
24
32
40
48
56
64
40
36
32
28
24
20
16
12
8
4
m

A2

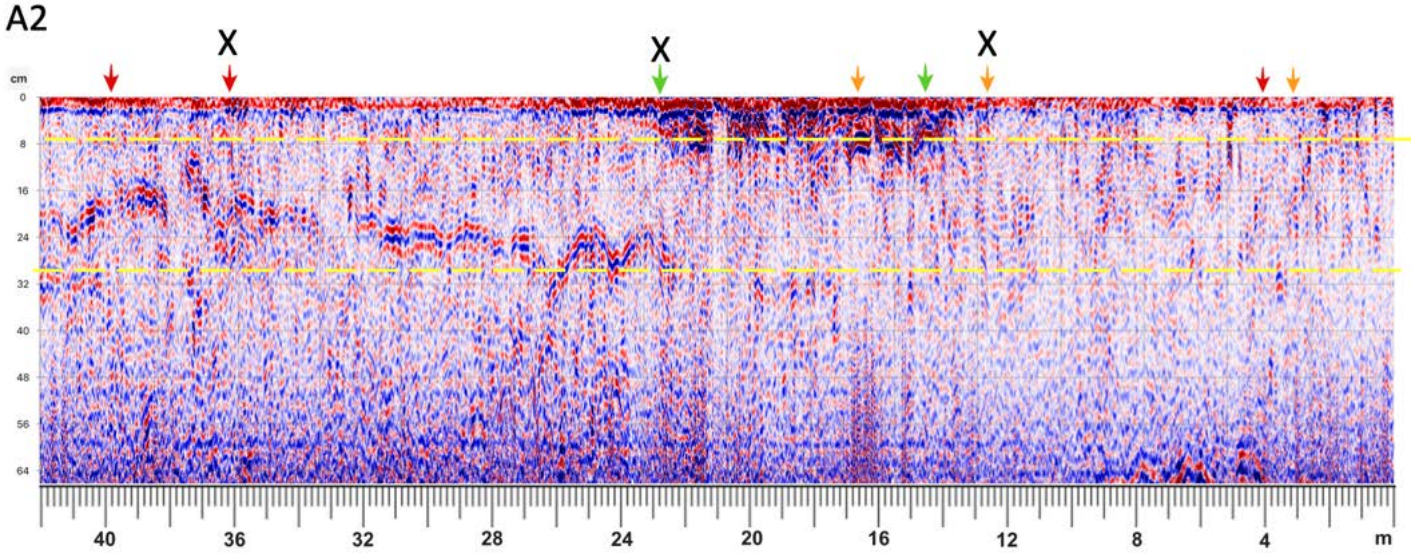
X
X
X
cm
0
8
16
24
32
40
48
56
64
40
36
32
28
24
20
16
12
8
4
m

A3

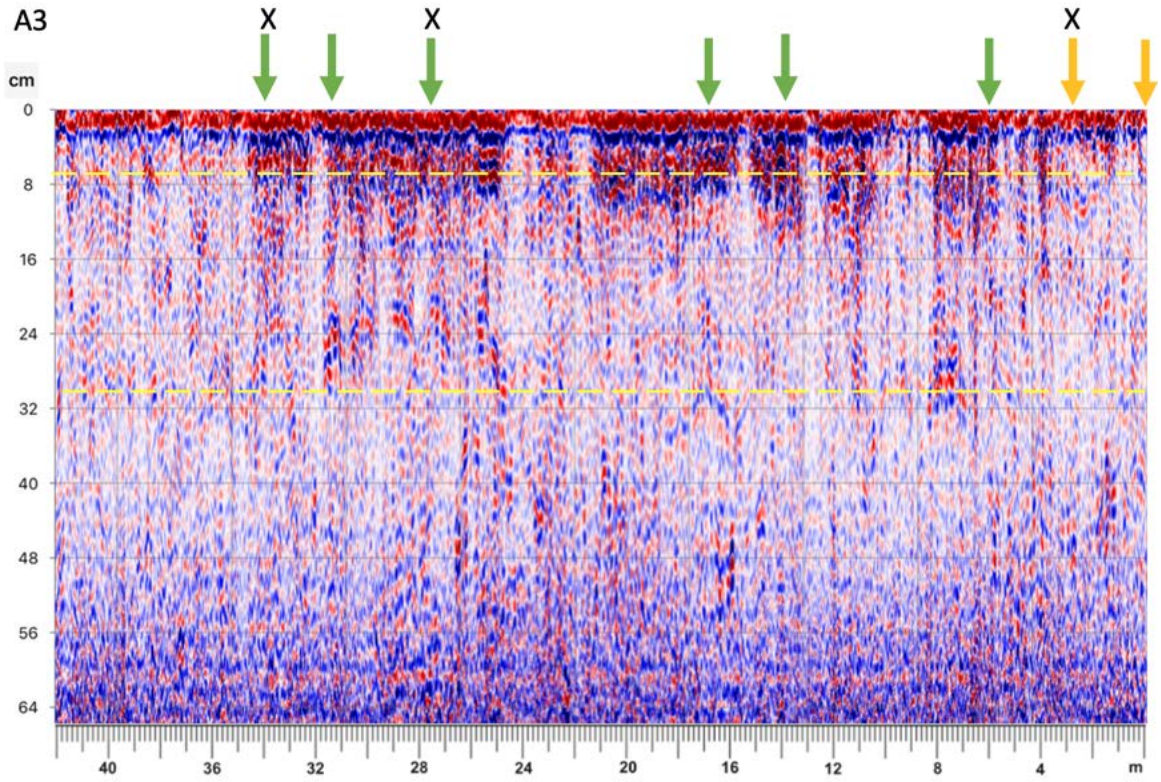
X
X
X
cm
0
8
16
24
32
40
48
56
64
40
36
32
28
24
20
16
12
8
4
m

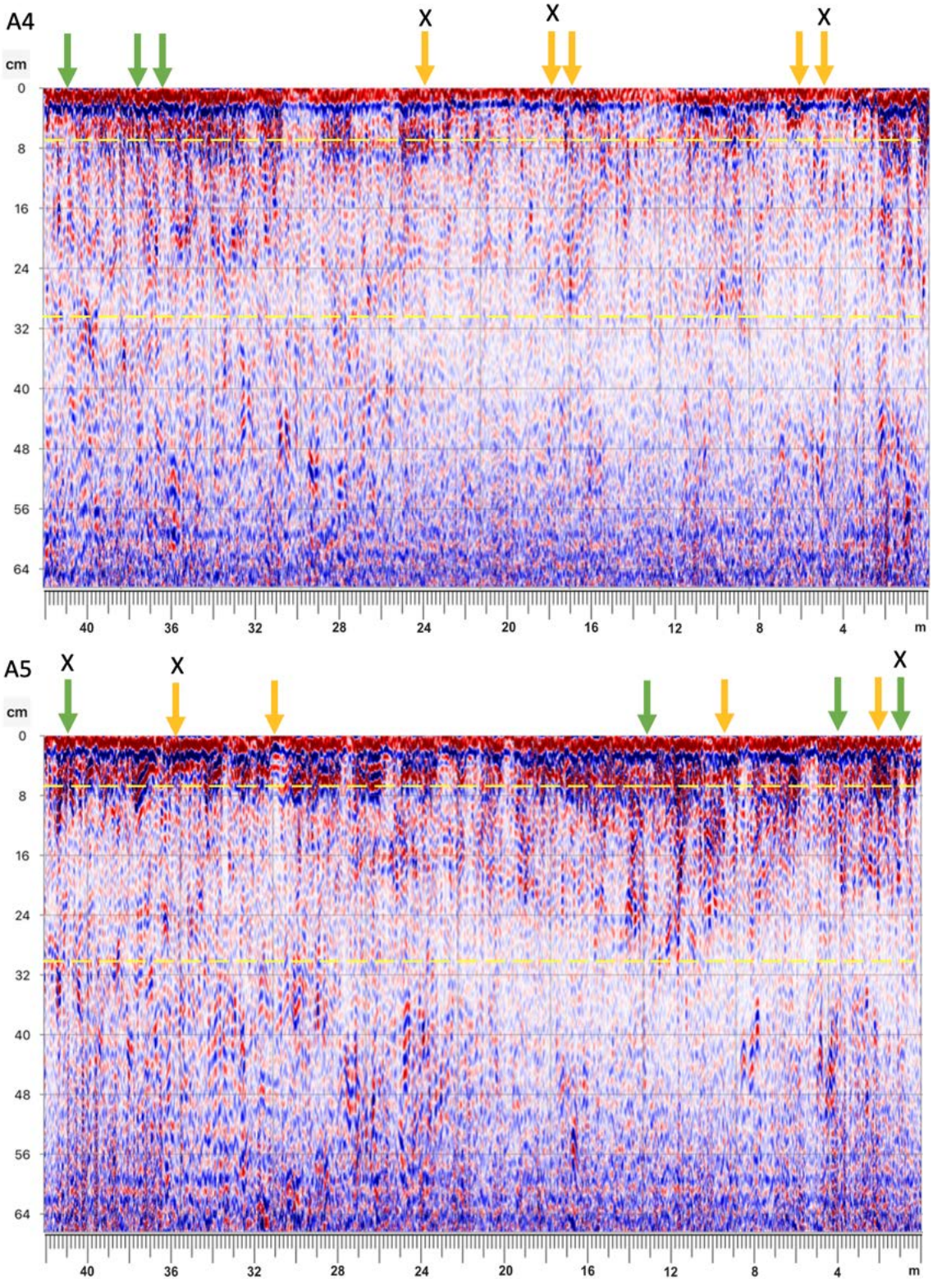
A4
X
X
X
cm
0
8
16
24
32
40
48
56
64
40
36
32
28
24
20
16
12
8
4
m
A5
X
X
X
cm
0
8
16
24
32
40
48
56
64
40
36
32
28
24
20
16
12
8
4
m

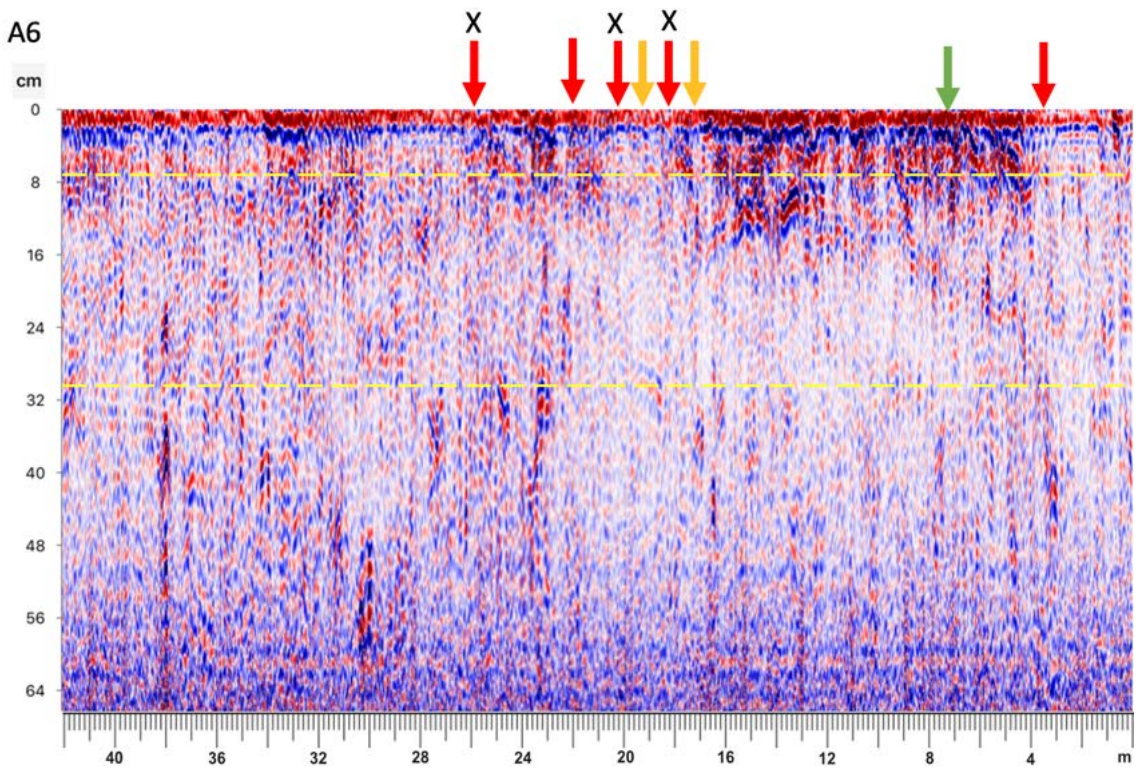
A6
cm
0
8
16
24
32
40
48
56
64
X
X
X
40
36
32
28
24
20
16
12
8
4
m